14 Oil Spill Remote Sensing: A Forensic Approach

Merv Fingas and Carl E. Brown

Emergencies Science and Technology Division, Environment Canada, Environmental Technology Centre, Ottawa, Ontario, Canada K1A 0H3.

14.1 Introduction

Spills of oil and related petroleum products in the marine environment can have serious biological and economic impacts (Wiese, 2002; Wiese and Ryan, 2003; Wiese et al., 2004). Public and media scrutiny is usually intense after a spill, with demands that the source of the oil spill be determined and the responsible party be brought to justice. Remote sensing is playing an increasingly important role in oil spill response efforts and will no doubt play an important role in forensics related to identifying "mystery spills" or discharges at sea. Through the use of modern remote sensing instrumentation, oil spillage can be monitored on the open ocean around the clock. Certain developments, particularly that of the laser fluorosensor, can provide enough forensic evidence to confirm that oil has indeed been spilled and that it is of a given type.

Even though the design and electronics of sensors are becoming increasingly sophisticated and sensors are becoming much less expensive, the operational use of remote sensing equipment lags behind the development of the technology. The most common forms of oil spill surveillance and mapping are done with simple still or video photography, which provide little, if any, forensic data. Remote sensing from an aircraft is still the most common form of oil spill tracking. Attempts to use satellite remote sensing for oil spills, although successful, are not necessarily as claimed and are generally limited to identifying features at sites of known oil spills. Forensic capability is not as good from satellite systems as from aircraft.

Several general reviews of oil spill remote sensing have been prepared (Fingas and Brown, 2000a, b, 2002a, 2005). These reviews show that progress is being made in oil spill remote sensing, although the progress is slow. The reviews also show that off-the-shelf sensors have very limited forensic application to oil spills, whereas specialized sensors offer advantages to oil spill remote sensing and an evolving forensic capability. Remote sensors for forensic application to oil spills are reviewed in this chapter. Many common sensors are available; however, they have limited forensic application. An infrared camera or an infrared/ultraviolet (IR/UV) system can detect oil under a variety of conditions and distinguish oil from some backgrounds but has limited forensic application. The inherent weaknesses of these systems include the inability to distinguish oil on beaches and among weeds or debris and to detect oil under certain lighting conditions. Lack of positive discrimination between oil and some backgrounds implies a lesser forensics applicability.

The laser fluorosensor is a most useful instrument to forensics because of its unique capability to positively identify oil against most backgrounds, including water, soil, weeds, ice, and snow. The availability of a fluorescent spectrum further enhances the forensic capability, particularly for identifying light oils that have different features.

Radar offers the only potential for searching in large areas and carrying out remote sensing during foul weather conditions, but offers very poor positive detection characteristics and thus low forensic capability. In addition, radar is prone to numerous interferences and false targets can be as high as 95%.

Equipment that measures relative slick thickness is still under development. Passive microwave has been studied for several years, but many commercial instruments lack sufficient spatial resolution to be practical, operational instruments. A prototype laser-acoustic instrument has been developed that provides the only technology to measure absolute oil thickness, but it may be too early to assess its potential for use in forensics. However, estimating spill volumes from slick thickness can have forensic implications.

Equipment operating in the visible spectrum, such as cameras and scanners, is useful for documentation or to provide a basis for the overlay of other data. This is the traditional forensic approach material; however, it is largely reliant on an expert observer rather than the discriminating power of the sensor and its output. It must be noted that oil shows no distinguishing spectral characteristics in the visible region; thus, documentation is by visual characteristics only.

Satellite-borne sensors are useful, particularly radar; however, their frequency of overpass and low spatial resolution make them of marginal use for spills. Radar satellites have similar forensic limitations as their airborne counterparts.

Sensors for detecting oil in ice are new and there are some promising concepts that require further research. Their potential for use in forensics, however, remains unknown at this time.

14.2 Visible Indications of Oil

Traditionally, much of the forensic work has been carried out by an "expert" observer trained to judge oil from its appearance and relate this to a vessel either discharging this oil or very close to where the oil was discharged. Often, however, oil on the water's surface is not visible to the eye (Fingas et al., 1999). Other than the obvious conditions of nighttime and fog, there are many other circumstances when oil cannot be seen. For example, oil is difficult to see if it is a thin slick such as from ship discharges or if it is masked by other materials on the water surface such as seaweed, ice, and floating debris. Often there are conditions or substances on the sea that may appear to be oil, but actually are not. These include wind shadows from land forms, surface wind patterns on the sea, surface dampening by submerged objects or weed beds, natural oils or biogenic material, and oceanic fronts. With large oil spills, the area covered by oil may be too great to be mapped visually. Due to all these factors, more sophisticated remote sensing systems must be used to assist in locating and tracking oil for forensic purposes.

14.3 Optical Sensors

14.3.1 Visible

Human vision alone is still the most common technique for oil spill surveillance and delivery of forensic evidence. In the past, major campaigns using only human vision were carried out with varying degrees of success (Taft et al., 1995). Optical techniques using the same range of the visible spectrum are the most common means of remote sensing. Cameras, both still and video, are common because of their low price and commercial availability. Documentation by camera images still forms the pillar of forensic evidence in court cases on oil discharges. Typically, these are presented by an expert observer who interprets the evidence to the court.

In recent years, visual and camera observation has been enhanced by the use of GPS (Global Positioning Systems) (Lehr, 1994). Systems are now available to directly map remote sensing data onto base maps.

In the visible region of the electromagnetic spectrum (approximately 400 to 700 nm), oil has a higher surface reflectance than water, but shows limited nonspecific absorption tendencies. Oil generally manifests throughout the entire visible spectrum. Sheen shows up silvery and reflects light over a wide spectral region down to the blue. As there is no strong information in the 500- to 600-nm region, this region is often filtered out to improve contrast (O'Neil et al., 1983). Overall, however, oil has no specific characteristics that distinguish it from the background (Brown et al., 1996).

Taylor studied oil spectra in the laboratory and the field and observed flat spectra with no usable features distinguishing it from the background (Taylor, 1992). Therefore, techniques that separate specific spectral regions within the visible spectrum do not increase detection capability. It has been found that high contrast in visible imagery can be achieved by setting the camera at the Brewster angle (53° from vertical) and using a horizontally aligned polarizing filter that passes only that light reflected from the water surface. This is the component that contains the information on surface oil (O'Neil et al., 1983). It has been reported that this technique increases contrast by up to 100%. Filters with bandpass below 450 nm can be used to improve contrast. These techniques, however, do not result in imagery that proves that oil is present nor can they define any physical or chemical characteristics of the oil.

On land, hyperspectral data (use of multiple spectral bands, typically 10 to 100) have been used to delineate the extent of an oil well blowout (Bianchi et al., 1995). The technique used was spectral reflectance in the various channels as well as the usual black coloration. This would provide some benefit in discriminating oil from land, but would not provide additional discrimination at sea.

Video cameras are often used in conjunction with filters to improve the contrast in a manner similar to that noted for still cameras. This technique has had limited success for oil spill remote sensing because of poor contrast and lack of positive discrimination. Despite this, video systems have been proposed as remote sensing systems for monitoring oil spills (Bagheri et al., 1995).

Scanners have been used as sensors in the visible region of the spectrum. A rotating mirror or prism sweeps the field-of-view (FOV) and directs the light toward a detector. Before the advent of CCD (charge-coupled device) detectors, this sensor provided much more sensitivity and selectivity than a video camera. Another advantage of scanners is that signals are digitized and processed before display. Newer technology now allows similar digitization to be achieved without scanning by using a CCD imager and continually recording all elements, each of which is directed to a different field-of-view on the ground. This type of sensor, known as a push-broom scanner, has many advantages over the older types. It can overcome several types of aberrations and errors, the units are more reliable than mechanical ones, and all data are collected simultaneously for a given line perpendicular to the direction of the aircraft's flight.

Several types of scanners were developed. In Canada, the MEIS (Multi-Detector Electro-optical Imaging Scanner) (O'Neil et al., 1983) and the CASI (Compact Airborne Spectrographic Imager) (Palmer et al., 1994) have been developed, and the Caesar system was developed in the Netherlands (Wadsworth et al., 1992). The CASI is now a commercial unit.

The use of visible techniques in oil spill remote sensing is largely restricted to documentation of the spill because there is no mechanism for positive oil detection and there are many interferences or false alarms. Sun glint and wind sheens can be mistaken for oil sheens. Biogenic material such as surface seaweeds or sunken kelp beds can be mistaken for oil. Oil on shorelines is difficult to identify positively because seaweeds look similar to oil and oil cannot be detected on darker shorelines.

In summary, the usefulness of the visible spectrum for oil detection is limited. It is, however, an economical way to document oil spills and provide baseline data on shorelines or relative positions. As there is no spectrum associated with oil, there is less forensic application with photography or visible cameras than with other sensors that provide a spectral signature.

14.3.2 Infrared

Oil, which is optically thick, absorbs solar radiation and re-emits a portion of this radiation as thermal energy, primarily in the 8- to 14-μm region. In infrared (IR) images, thick oil appears hot, intermediate thicknesses of oil appear cool, and thin oil or sheens are not detected. The thickness at which these transitions occur is not well understood, but evidence indicates that the transition between the hot and cold layer is between 50 and 150 μm, and the minimum detectable layer is between 10 and 70 μm (Hurford, 1989; Goodman, 1989; Belore, 1982; Neville et al., 1979).

The reason for the appearance of the "cool" slick is not fully understood. A plausible theory is that a moderately thin layer of oil on the water surface causes destructive interference of the thermal radiation waves emitted by the water, thereby reducing the amount of thermal radiation emitted by the water (Fingas et al., 1999). This may be analogous to the appearance of the rainbow sheen, which is explained in Section 14.6.2. The cool slick would correspond to the thicknesses as observed above because the minimum destructive thickness would be about two times the wavelength, which is between 8 to 10 μm. This would yield a destructive onset of about 16 to 20 μm to about four wavelengths, or about 32 to 40 μm. The destructive area is usually only seen with test slicks, which is explained by the fact that the more rapidly spreading oil is more transparent than the remaining oil. In theory, the onset of the hot thermal layer would then be at thicknesses greater than this or at about 50 μm. Infrared sensors do not provide enough information to establish either the thickness or presence of oil on a forensic basis.

Infrared devices cannot detect emulsions (water-in-oil emulsions) under most circumstances (Bolus, 1996). This is probably due to the high thermal conductivity of emulsions as they typically contain 70% water and thus do not show a temperature difference.

Infrared cameras are now very common and commercial units are available from several manufacturers. Scanners with infrared detectors have been used recently. The older type of infrared detectors, however, required cooling to avoid thermal noise, which would overwhelm any useful signal. Liquid nitrogen, which provides about 4 hours of service, was traditionally used to cool the detector. New, smaller sensors use closed-cycle or Sterling coolers, which operate on the cooling effect created by an expanding gas. While a gas cylinder or compressor must be transported with this type of cooler, refills or servicing may not be required for days at a time (Goodman, 1988). In the past few years, uncooled detectors have entirely replaced the older, cooled detectors.

Most infrared sensing of oil spills takes place in the thermal infrared at wavelengths of 8 to 14 μm. One sensor, which is designed as a fixed-mounted unit, uses the differential reflectance of oil and water at 2.5 and 3.1 μm (Seakem Oceanography, 1988). Tests of a mid-band infrared system (3.4 to 5.4 μm) over the *Tenyo Maru* oil spill showed no detection in this range; however, ship scars were visible (Rogne and Smith, 1992; Rogne et al., 1992; Kennicutt et al., 1992). Specific studies in the thermal infrared (8 to 14 μm) show that there is no useful spectral structure in this region (Salisbury et al., 1993). Tests of a number of infrared systems show that spatial resolution is extremely important when the oil is distributed in windrows and patches, emulsions are not always visible in the IR, and cameras operating in the 3- to 5-μm range are only marginally useful (Hover, 1994).

The relative thickness information in the thermal infrared can be used to direct countermeasures equipment to thicker portions of the oil slick, but is not useful forensically. Oil detection in the infrared is not positive, however, as several false targets can interfere, including seaweed, shoreline, and oceanic fronts (Brown et al., 1998). Thus, the presence or absence of infrared spectral information about spilled oil has limited application in a forensic sense.

14.3.3 Ultraviolet

Ultraviolet sensors can be used to map sheens of oil, as oil slicks display high reflectivity of ultraviolet (UV) radiation even at thin layers (<0.1 μm). Overlaid UV and IR images are often used to produce a relative thickness map of oil spills. Although inexpensive, ultraviolet cameras are not often used in this process, however, as it is difficult to overlay camera images (Goodman, 1988). Data from infrared scanners and that derived from push-broom scanners can be easily superimposed to produce these IR/UV overlay maps. Ultraviolet data are also subject to many interferences or false images such as wind slicks, sun glints, and biogenic material. Since these interferences are often different than those for infrared sensing, combining IR and UV can provide a more positive indication of oil than using either technique alone, but does not offer high forensic proof.

14.3.4 Night Vision Cameras

The night vision camera has the ability to capture the image of the water's surface under low light levels such as would be expected on a clear, starlit night. Oil is not positively detected using this technology, but it might be possible to discern a contrast between oil and the surrounding water.

With new light-enhancement technology (low lux), video cameras can be operated even in darkness. Tests of a Generation III night vision camera show that this technology is capable of providing imagery in very dark night conditions (Brown et al., 2004a, 2005a). Earlier, low-light level cameras were used for this purpose, but they required at least moonlight to produce an image (O'Neil et al., 1983). Under very low-light level conditions, the Generation III night vision camera now in use has enough sensitivity to observe the ultraviolet laser pulses from the Scanning Laser Environmental Airborne Fluorosensor (SLEAF) on the water's surface. Furthermore, it is postulated that it should be possible to observe visible fluorescence induced by the SLEAF ultraviolet laser if oil is present on the surface. This would be observable as brighter spots on the surface.

In 1993, a less advanced unit (Generation II) was used to image oil in shallow manmade pools onto which oil was deposited (Hover and Plourde, 1994). Although a contrast was observed between the oil and water, it was suspected that some of the contrast was due to the shallow depth of the pools and might not be evident in deeper waters.

A night vision camera may provide substantiating imagery similar to cameras and other photographic devices. The application of this technology to oil spill detection has not been studied extensively.

14.4 Laser Fluorosensors

Laser fluorosensors are active sensors that take advantage of the fact that certain compounds in petroleum oils absorb UV light and become electronically excited. This excitation is rapidly removed through the process of fluorescence emission, primarily in the visible region of the spectrum. Since very few other compounds show this tendency, fluorescence is a strong indication of the presence of oil. Natural fluorescing substances, such as chlorophyll, fluoresce at sufficiently different wavelengths than oil to avoid confusion.

As different types of oil yield slightly different fluorescent intensities and spectral signatures, it is possible to differentiate between classes of oil under ideal conditions (Balick et al., 1997; Brown and Fingas, 2003; Brown et al., 1994a, 2001a, 2002a, b, 2003a, b, 2004a, b, 2005a; Hengstermann and Reuter, 1990; Pantani et al., 1995). Laser fluorosensors are the most important sensor in terms of the forensics of oil spill detection as they provide positive detection capability, a classification, and, most importantly, a spectrum, which is somewhat akin to a gas chromatogram (i.e., a chemical fingerprint).

Another phenomenon, known as Raman scattering, involves energy transfer between the incident light and the water molecules. When the incident UV light interacts with the water molecules, Raman scattering occurs. The water molecules absorb some of the energy as rotational-vibrational energy and scatter light at wavelengths that are the difference between the incident radiation and the vibration-rotational energy of the molecule. The Raman signal for water occurs at 344 nm when the incident wavelength is 308 nm (XeCl laser). The water Raman signal is useful for maintaining wavelength calibration of the fluorosensor in operation, but has also been used in a limited way to estimate oil thickness (thicknesses less than 10 μm depending on the oil type) because the strong absorption by oil on the surface will suppress the water Raman signal in proportion to thickness (Hoge and Swift, 1980; Piskozub et al., 1997). This is shown in Eq. (14-1).

$$\text{transmittance} = \text{EXP}\ (\text{thickness} \times \text{absorption coefficient}) \qquad (14\text{-}1)$$

The point at which the Raman signal is entirely suppressed depends on the type of oil, since each oil has a different absorption coefficient. Details of the use of Raman scattering to measure oil slick thickness can be found in the early work of Hoge and Swift (1980) and the recent studies by Patsayeva et al. (2000).

The principle of fluorescence can also be used on a smaller scale. A handheld UV light has been developed to detect oil spills at night at short range (Fingas, 1982). The "Fraunhofer Line Discriminator" is another related instrument, which is essentially a passive fluorosensor using solar irradiance instead of laser light (O'Neil et al., 1983). This instrument was not very successful because of the limited discrimination and the low signal-to-noise ratio.

Laser fluorosensors have been developed over the past 30 years to allow for the exploration of petroleum resources and the airborne surveillance and monitoring of oil spills. The first airborne laser fluorosensors were flown in the early 1970s, including those in Ottawa reported in Measures and Bristow (1971). Another pioneering development was NASA's Airborne Oceanographic Lidar, details of which can be found on its website (NASA, 2001).

Laser fluorosensors are active sensors that provide their own source of excitation and can therefore operate equally well during full daylight conditions and at night. The high sensitivity of many of these instruments allows even small amounts of the fluorescent substances, e.g., petroleum oils, being investigated to be detected. Recently, the ability to deal with the large quantities of data collected by laser fluorosensors has improved dramatically. True real-time operating systems and the increased processing power provided by modern computer processors can produce usable data in real time on-board the aircraft. In the case of a response to an oil spill situation, fluorescence information can be rapidly transferred to personnel on the ground or at sea to aid in the effective interdiction of any polluter.

Most laser fluorosensors used for oil spill detection employ an ultraviolet laser emitting between 300 and 355 nm (Anderson, 1994; Barbini et al., 1991; Brown et al., 1996; Calleri and Bernardi, 1993; Castagnoli et al., 1986; Diebel et al., 1989; Geraci et al., 1993; Gruner et al., 1991; Koechler et al., 1992). These excitation wavelengths are a compromise in that they can excite all three classes of oil with reasonable efficiency. Shorter-wavelength lasers would excite lighter oils efficiently but are less efficient at exciting crude and heavy refined oils. Figure 14-1 shows the discrimination in spectra obtained using a fluorosensor targeting three fuels with nearly identical physical properties. Such discrimination is not the case with heavier oils.

There are several reasonably priced, commercially available ultraviolet lasers in the 300- to 355-nm region, including the XeCl excimer laser (308 nm), the nitrogen laser (337 nm), the XeF excimer laser (351 nm), and the frequency-tripled Nd:YAG (355 nm). With excitation in this wavelength region, there exists a spectrally broad fluorescent return due

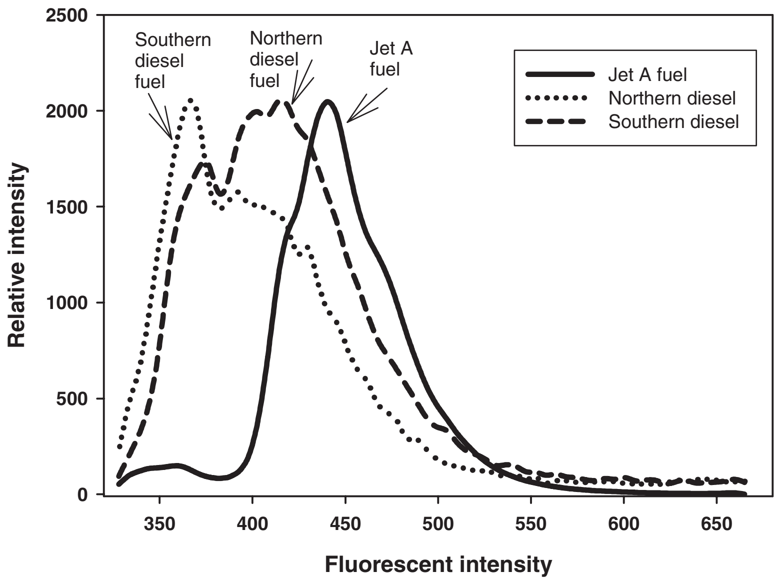

Figure 14-1 Spectra of three fuels with similar physical properties showing the spectral differences in them using a fluorosensor.

to organic matter, centered at 420 nm. This is known as Gelbstoff or yellow matter and must be accounted for. The signal due to Gelbstoff disappears when the oil layer is optically thick (10 to 20 μm). It can, however, be an interfering signal when attempting to detect thin films of light oils on water. Chlorophyll yields a sharp peak at 685 nm. Typically, crude oil fluorescence return is in the region of 400 to 550 nm, with the maximum centered in the 480-nm region.

Laser fluorosensors have significant potential for the remote sensing of petroleum oils because they can discriminate between oiled and unoiled weeds and detect oil in a variety of marine and terrestrial environments including on water, snow, ice, and beaches. Tests on shorelines show that this technique has been very successful (Dick et al., 1992). This coupled with their forensic capability extends the capability to shoreline and land as well as at sea.

Algorithms have been developed for the detection of oil on shorelines (James and Dick, 1996). Work has been conducted on detecting oil in the water column such as occurs with the product Orimulsion (Brown et al., 2002b, 2003a, b). The fluorosensor is also the only reliable means of detecting oil in certain ice and snow situations. Recent usage shows that the laser fluorosensor is a powerful tool for oil spill remote sensing for forensic purposes (Brown et al., 1997a).

Environment Canada's current system, the Scanning Laser Environmental Airborne Fluorosensor (SLEAF), was designed to detect, characterize, and map oil contamination in marine coastal and shoreline environments (Brown et al., 2000). Excitation is provided by a 100-mJ/pulse, 308-nm XeCl excimer laser (Lambda Physik, LPX140i) operating at rates of up to 400 Hz. Laser-induced fluorescence is detected with a spectrometric receiver consisting of a 20-cm-diameter, *f*/3 Newtonian telescope, with a 1 × 3-mrad field-of-view, a concave holographic grating, and a gated intensified diode-array detector (Princeton Instruments, 64 spectral channels, 330 to 610 nm). The detector is range-gated with digital lidar circuitry in order to collect only the laser-induced fluorescence, while rejecting most of the background solar radiation.

Two scanner heads (Optech Inc.) are used to provide a choice of narrow or wide swath coverage (1/6 or 1/3 of the operating altitude of 300 to 600 m). Full spectral resolution georeferenced, fluorescence data are collected for each laser pulse and recorded directly to computer hard disk. Individual fluorescence spectra are analyzed in real time to determine the presence or lack of oil in the sensor field-of-view. Oil is classified using a principal component analysis (James and Dick, 1996) as light, medium, or heavy, and the extent of oil coverage in the field-of-view is estimated as clean, light, moderate, or heavy.

Oil contamination is displayed on the operator's display monitor and on hard-copy maps. Oil class is illustrated on the operator's display by color and with a text message on the hard-copy map. Oil coverage is represented by the length of a line perpendicular to the flight path of the aircraft. Since the amount of oil classification and coverage information is considerable, results are averaged over an area approximately 50 m long by one-half of the swath width on either side of the aircraft. This averaging allows for a more concise and readable summary of oil contamination on the map display.

14.5 Microwave Sensors

14.5.1 Radiometers

Microwave radiometers detect the presence of an oil film on water by measuring an interference pattern excited by the radiation from free space. The apparent emissivity factor of water is 0.4 compared to 0.8 for oil (O'Neil et al., 1983; Ulaby et al., 1989). A passive device can detect this difference in emissivity and could therefore be used to detect oil. In addition, as the signal changes with thickness, in theory, the device could be used to measure thickness.

This detection method has not been very successful in the field, however, as several environmental and oil-specific parameters must be known. In addition, the signal return is dependent on oil thickness but in a cyclical fashion. A given signal strength can imply any one of two or three signal film thicknesses within a given slick. Microwave energy emission is greatest when the effective thickness of the oil equals an odd multiple of one-quarter of the wavelength of the observed energy. Biogenic materials also interfere, and the signal-to-noise ratio is low. In addition, it is difficult to achieve high spatial resolution (Goodman, 1994a).

The Swedish space agency has done some work with different systems, including a dual-band, 22.4- and 31-GHz device and a single-band 37-GHz device (Fäst, 1986). A two-channel device operating at 37.5 and 10.7 GHz is described in Skou et al. (1994). Mussetto and coworkers described the tests of 44- to 94-GHz and 94- to 154-GHz, two-channel devices over oil slicks (Mussetto et al., 1994). They showed that correlation with slick thickness is poor and suggest that factors other than thickness also change surface brightness. They suggest that a single-channel device might be useful as an all-weather, relative-thickness instrument.

Tests of single-channel devices over oil slicks have also been described in the literature, specifically a 36-GHz (Zhifu and Wiesbeck, 1988) and a 90-GHz device (Süss et al., 1989). A new method of microwave radiometry has recently been developed in which the polarization contrasts at two orthogonal polarizations are measured in an attempt to measure oil slick thickness (Pelyushenko, 1995, 1997). A series of frequency-scanning radiometers have been built and appear to have overcome the difficulties with the cyclical behavior (McMahon et al., 1995, 1997).

In summary, passive microwave radiometers may have potential as all-weather oil sensors. Their potential as a reliable device for measuring slick thickness, however, is uncertain at this time, and thus their forensic application is limited.

14.5.2 Radar

Capillary waves on the ocean reflect radar energy, producing a "bright" image known as sea clutter. Since oil on the sea surface dampens some of these capillary waves, the presence of an oil slick can be detected as a "dark" sea or one with an absence of this sea clutter. Unfortunately, oil slicks are not the only phenomena that are detected in this way. There are many interferences or false targets, including fresh water slicks, wind slicks (calms), wave shadows behind land or structures, seaweed beds that calm the water just above them, glacial flour, biogenic oils, and whale and fish sperm (Frysinger et al., 1992; Hühnerfuss et al., 1989; Poitevin and Khaif, 1992). As a result, radar can be ineffective in locations such as Prince William Sound, Alaska, where dozens of islands, freshwater inflows, ice, and other features produce hundreds of such false targets. Its forensic capability is therefore low. Despite these limitations, radar is an important tool for oil spill remote sensing because it is the only sensor that can be used to search large areas and it is one of the few sensors that can "see" at night and through clouds or fog.

The two basic types of radar that can be used to detect oil spills and for environmental remote sensing in general are synthetic aperture radar (SAR) and side-looking airborne radar (SLAR). The latter is an older, but less expensive, technology, which uses a long antenna to achieve spatial resolution. Synthetic aperture radar uses the forward motion of the aircraft to synthesize a very long antenna, thereby achieving very good spatial resolution, which is independent of range, but with the disadvantage of requiring sophisticated electronic processing.

While inherently more expensive, the SAR has greater range and resolution than the SLAR. In fact, comparative tests show that SAR is vastly superior (Bartsch et al., 1987; Brown and Fingas, 2003b; Mastin et al., 1994). Search radar systems, such as those frequently used by the military, cannot be used for oil spills as they usually remove the clutter signal, which is the primary signal of interest. Furthermore, the signal processing of this type of radar is optimized to pinpoint small, hard objects, such as periscopes. This signal processing is very detrimental to oil spill detection.

SLAR has predominated oil spill remote sensing, primarily because of its lower price (Dyring and Fäst, 2004; Zielinski and Robbe, 2004). Operators recognize that SLAR is very susceptible to false hits, but solutions are not offered. SLAR is not typically used for forensic purposes, but rather is used to provide wide swath-width detection.

Experimental work on oil spills has shown that X-band radar yields better data than L- or C-band radar (C-CORE, 1981; Intera Technologies, 1984). It has also been shown that vertical antenna polarizations for both transmission and reception (V,V) yield better results than other configurations (Bartsh et al., 1987; Kozu et al., 1987; Macklin, 1992; Madsen et al., 1994). The ability of radar to detect oil is also limited by sea state. Sea states that are too low will not produce enough sea clutter in the surrounding sea to contrast to the oil, and very high seas will scatter radar sufficiently to block detection inside the troughs. Indications are that minimum wind speeds of 1.5 m/s (~3 knots) are required to allow detectability, and a maximum wind speed of 6 m/s (~12 knots) will again remove the effect (Hühnerfuss et al., 1996; Hielm, 1989). This limits the environmental window of application for using radar to detect oil slicks.

Gade et al. (1996) studied the difference between extensive systems from a space-borne mission and a helicopter-borne system. They found that at high winds, it was not possible to discriminate biogenic slicks from oil. At low wind speeds, it was found that images in the L-band showed discrimination. Under these conditions, the biogenic material showed greater damping behavior in the L-band. Okamoto et al. (1996) studied the use of ERS-1 using artificial oil (oleyl alcohol) and found that an image was detected at a wind speed of 11 m/s but not at 13.7 m/s.

Radar has also been used to measure currents and predict oil spill movements by observing frontal movements (Forget and Brochu, 1996). Work has shown that frontal currents and other features can be detected by SAR (Marmorino et al., 1997).

Shipborne radar has similar limitations and the additional handicap of low altitude, which restricts its range to 8 to 30 km, depending on the height of the antenna. Ship radars can be adjusted to reduce the effect of sea clutter de-enhancement. Shipborne radar successfully detected a surface slick in the Baltic Sea from 8 km away and during a trial off the coast of Canada at a maximum range of 17 km (Tennyson, 1985). During the *Prestige* spill, a Netherlands vessel successfully used this technique to guide a recovery vessel into slicks. The technique is, however, very limited by sea state and, in all cases where it was used, the presence and location of the slick were already known or suspected. Ship radars will provide little forensic evidence.

Gangeskar (2004) has proposed an automatic system that could be mounted on oil-drilling platforms. This system would use standard X-band ship navigation units and provide an alert if an oil spill is present. The system includes an extensive post-processing system to provide both a user-friendly GUI (graphical user interface) and an automatic detection and alert system. The system has not been fully tested to date.

In summary, radar optimized for oil spills is useful in oil spill remote sensing, particularly for searches of large areas and for nighttime or foul weather work. The technique is highly prone to false targets, however, and is limited to a narrow range of wind speeds. Radar therefore offers little in the way of forensic data.

14.5.3 Microwave Scatterometers

A microwave scatterometer measures the scattering of microwave or radar energy by a target. The presence of oil reduces the scattering of the microwave signals just as it does for radar sensors, however, and this device is adversely affected by the same large number of false targets. One radar scatterometer was flown over several oil slicks and used a low-power transmitter operating in the Ku band (13.3 GHz) (O'Neil et al., 1983). The scatterometer detected the oil, but discrimination was poor. The "Heliscat," a device with five frequencies, has been used to investigate capillary wave damping (Hühnerfuss et al., 1996).

The advantage of a microwave scatterometer is that it has an aerial coverage similar to optical sensors and it operates in a nadir geometry, i.e., it looks straight down. The main disadvantages include the lack of discrimination for oil and the lack of imaging capability. As with radar, there is little of relevance for forensic applications.

14.6 Determination of Slick Thickness

There are presently no reliable methods, either in the laboratory or in the field, for accurately measuring the thickness of an oil slick on water. There has long been a need to measure the thickness of oil slicks, both within the oil spill response community and among academics in the field. Knowledge of slick thickness would make it possible to determine the effectiveness of certain oil spill countermeasures including dispersant application and *in situ* burning. Indeed, the effectiveness of individual dispersants could be determined quantitatively if the oil remaining on the water surface after dispersant application could be accurately measured (Goodman and Fingas, 1988). The knowledge of oil spill thickness may also be useful in forensic applications, as the quantity of oil at sea is often a relevant issue in court. The quantity of oil can only be estimated if a reliable estimate or measurement of oil thickness is available.

14.6.1 Visual Thickness Indications

A very important tool for working with oil spills has been the relationship between appearance and thickness. A series of experiments were conducted in the 1930s, and charts produced then are still used today (Congress, 1930). It had already been recognized that slicks on water were consistent or nearly consistent in appearance. Only a few experiments have been done in recent years.

14.6.2 Theoretical Approaches

Horstein (1972, 1973) reviewed theoretical approaches and used interference phenomenon to correlate the threshold of rainbow colors to slick thickness. The appearance of the rainbow colors is the result of constructive and destructive interference of the lightwaves reflected from the air–oil interface with those reflected from the oil–water interface. The difference in optical path lengths for these two waves depends on the refractive index of the oil. The refractive index of a given wavelength results in a difference in optical path length. This difference can be given as

$$\Delta L = 2t\,(\mu^2 = \sin^2 i)^{1/2} \qquad (14\text{-}2)$$

where

ΔL is the difference in optical path length
t is the film thickness
μ is the refractive index of the film
i is the angle of light incidence

Horstein points out that if ΔL contains a whole number of wavelengths, then maximum destructive interference will occur. If ΔL contains an odd number of half-wavelengths, then maximum constructive interference will occur.

Then the maximum destructive interferences occur at

$$\lambda = \Delta L/x \qquad (14\text{-}3)$$

where λ is the wavelength under consideration, and x is a whole even number such as 2, 4, 6, etc. The maximum constructive interferences occur at

$$\lambda = 2\Delta L/x \qquad (14\text{-}4)$$

where x is a whole odd number such as 1, 3, 5, 7, etc.

Tables of constructive and destructive wavelengths can be written. These then result in the following color chart for visible oil:

thickness less that 0.15 µm — no color apparent
thickness of 0.15 µm — warm tone apparent
thickness of 0.2 to 0.9 µm — variety of colors (e.g., rainbow)
thickness greater than 0.9 µm — colors of less purity, heading toward gray

Horstein calculated the differential reflectivity of oil and water. He calculated that, at an incidence angle of 30°, the reflectivity of oil is 0.041 and that of water is 0.021. At 60° oil shows a reflectivity of 0.09 and water of 0.06 and at 75° oil has a reflectivity of 0.25, and water that of 0.21. These angles are calculated as the angle of light incidence from the normal and thus show that reflectivity decreases as the angle of viewing becomes less vertical. The reflectivity may explain the visibility of very thin films of oil (less than shown by coloration) on the water surface. This calculation demonstrates that viewing angle is important and that the greatest contrast is seen from near-vertical angles.

14.6.3 Literature Review of Visual Indications of Oil Slick Thickness

Literature results are presented in chronological order and numerical values are summarized in Table 14-1. In 1930, scientists from the U.S. Navy and the National Bureau of Standards conducted both laboratory and field studies to examine the visibility and fate of oil slicks (Congress, 1930). Oil was spilled near Hawaii and off New York, and then followed until it was no longer visible. Weather, area, etc. were recorded. It was concluded that the minimum visible thickness of an oil slick is 0.1 µm.

Allen and Schlueter (1969, 1970) developed a slick thickness algorithm for the purpose of estimating the discharges from the Santa Barbara oil seeps. In 1969, the American Petroleum Institute compiled a visibility chart using much of the previous literature (API, 1969). This chart has been used in many subsequent documents. Hollinger and Mennella (1973) conducted a series of eight controlled oil spills off the coast of Virginia to investigate the use of microwave radiometry to delineate oil spills. It was noted that the sheens were typically 2- to 4-µm thick. It was found that 90% of the oil was in 10% of the slick area. Horstein (1972) studied the relationship of slick

Table 14-1 Relationships between Appearance and Oil-Slick Thickness

Author	*Year*	*Oil*	*Type*	*Number*	*Height (m)*	*Viewing Angle*	*Visibility Thresholds (µm)*						*Other Information*
							Minimum	*Silvery*	*Rainbow*	*Darkening Colors*	*Dull Colors*	*Brown*	
Congress	1930	Various incl. Bunker, fuel oil	Experiments	>15	Ship board	Oblique	0.1						
Allen and Schlueter	1969	Crude—Santa Barbara	Experiments	Multiple	ns	ns		0.05 to 0.18	0.23 to 0.75	1 to 2.5	2.5 to 5.5		Probably done at close proximity
API	1969	General	Literature		ns	ns	0.04	0.08	0.15 to 0.3	1	2		
Horstein	1972	Arabian and Louisiana crudes	Experiments	>20	1 to 2	Various	<0.15	up to 0.15	0.15 to 0.9	0.9 to 1.5	1.5 to 3		
Horstein,	1973	Various	Lit & experiments		Ship & aerial	Various	0.038	0.076	0.15 to 0.31	1	2		
Parker, and Cormack	1979	North Sea and Arabian crudes	Experiments	2	Ship & aerial	Various	0.1						
ITOPF	1981	General	Literature		Aerial	ns	0.1	0.1	0.3	0.1			
Schriel	1987	General	Lit & experiments		Aerial	Various	0.05	0.1	0.15	0.3	1	2	Combination of experiments and literature
Schriel	1987	General	Lit & experiments		Aerial	Various		0.1	0.3	1	5	15	Modified table
Duckworth	1993	Various crudes	Experiments	Several	ns	ns	0.1	0.1	0.1 to 1				Wave dampening threshold at 0.1 µm
Brown et al.	1995	Crude—Norman Wells	Experiments	32	30 m	Nadir	0.094						
		Diesel	Experiments	25	30 m	Nadir	0.165						
		Lubricating oil	Experiments	16	30 m	Nadir	0.077						
		Hydraulic oil	Experiments	13	30 m	Nadir	0.159						
Coast Guard	1996	General—tar codes	Literature				0.04	0.075	0.15	0.3	1	3	
						Average	***0.09***	***0.1***	***0.59***	***0.91***	***2.7***	***8.5***	

ns = not specified

thickness and appearance theoretically and in the laboratory as well as from spills in the field. Horstein calculated that oil would show rainbow colors beginning at 200 nm (0.2 μm) on the basis of wave interference calculations. Onset of any color would be at 150 nm for the same reason.

In 1981, the International Tanker Owners Pollution Federation published a visibility guide based on existing literature (ITOPF, 1981). Schriel (1987) presented a table of thickness estimation based both on literature and on experiments conducted in the North Sea. MacDonald et al. (1993) used photography to define slicks in an area of the Gulf of Mexico, offshore from Louisiana. Work performed from the space shuttle, surface ships, aircraft, and a submarine confirmed oil in some of the slicks. In the case of the shuttle photography, pictures of the surface were best using the sun glint, i.e., when the sun was shining onto the surface creating the most glint. Unpublished thickness data, based on small-scale experiments and literature, were used to calculate the oil on the surface.

Brown et al. (1995, 1996) conducted 120 experiments in a large wave basin to measure the visibility of oil slicks. It was found that the detection ability decreased by over 50% for most oils and for the cameras when the angle was changed from 90° to 55° from the horizontal. Detectability degraded to 70% and sometimes to nil as the viewing angle was decreased past 55° through 35°. It is concluded that under optimal conditions, a sheen of about 0.15 μm can be detected visually. Sun angle is important, and it was found that the best angle is with the sun at right angles to the viewing plane. This degrades as viewing angle decreases and depends on oil type. The Canadian Coast Guard, as well as many other organizations around the world, has issued color charts for their operational personnel (Canadian Coast Guard, 1996). These data are based on many of the historical works described here.

On the basis of the literature results discussed in this section, it can be seen that visual or photographic evidence for slick thickness cannot be used outside the range of about 0.5 to 2 μm in the color regime.

14.6.4 Oil Slick-Thickness Relationships in Remote Sensors

Hollinger and Mennella (1973) conducted a series of eight controlled oil spills off the coast of Virginia to investigate the use of microwave radiometry to delineate oil spills. They used 19.4- and 69.8-GHz radiometers on the spills. Measurements using sorbents were used to calibrate the radiometer. It was noted that the sheens were typically 2- to 4-μm thick. It was found that 90% of the oil was in 10% of the slick area and that the microwave threshold was about 0.1 mm (100 μm).

A series of experiments were carried out in 1979 to evaluate infrared (IR) and side-looking airborne radar (SLAR) for oil spill detection (Parker and Cormack, 1979). The imagery was correlated against visual and sorbent measurements, which were used to derive a thickness estimate. It was concluded that the infrared threshold was between 25 and 50 μm, and 100 nm for SLAR. Manipulation of data showed that a mass balance could be achieved if the thickness at which the infrared showed oil to be colder at the sea occurred at 100 μm and at 1000 μm for the heated portion of the oil.

The United Kingdom conducted Isowake Experiments in 1982 (Hurford and Martinelli, 1982, 1984). On the basis of estimations and calculations, it was concluded that the lowest detectable slick thickness for IR was between 10 and 50 μm, whereas hot spots in the IR image could be as much as 1000 μm.

MacDonald et al. (1993) used photography from the space shuttle to define up to 124 slicks in an area of the Gulf of Mexico, offshore from Louisiana. Similarly, a thematic image from Landsat showed at least 66 slicks in one large area. Some of the thickness relationships were based on unpublished experimental data from Duckworth (1993).

Brown et al. (1995, 1996) conducted experiments to measure the visibility of oil slicks. The observers and an ultraviolet and visible camera were mounted in a crane basket 30 m over the slick. It was found that the detection ability decreased by over 50% for most oils and for the cameras when the angle was changed from 90° to 55° from the horizontal (equivalent incidence angle of 0° to 35°). Detectability degraded to 70% and sometimes to nil as the viewing angle was decreased past 55° through 35°. Brown et al. (1998) conducted several experiments to ascertain the relationship between thickness of slicks and the density (or intensity) of the infrared image. The thicknesses varied between 1 to 10 mm, and thicknesses were measured using an acoustic system. No relationship was found between slick thickness and infrared brightness.

The results of some of the experiments reviewed are summarized in Table 14-2.

It is readily apparent from the discussion in this section that most available oil spill remote sensors do not provide forensic-quality oil-thickness information. Furthermore, the thresholds for many of the sensors vary over two orders-of-magnitude.

14.6.5 Specific Oil-Thickness Sensors

The suppression of the water Raman peak in laser fluorosensor data discussed in Section 14.4 has not been fully exploited or tested. This technique may work for thin slicks, but not necessarily for thick ones, at least not with a single excitation frequency. Attempts have been made to calibrate the thickness appearance of infrared imagery, but also without success. It is suspected that the temperatures of the slick as seen in the IR are highly dependent on oil type, sun angle, and weather conditions. If so, it may not be possible to use IR as a calibrated tool for measuring thickness. As accurate ground-truth methods do not exist, it is very difficult to calibrate existing equipment. The use of sorbent techniques to measure surface thickness yields highly variable results (Goodman and Fingas, 1988). As noted in Section 14.5.1, the signal strength measured by microwave radiometers can imply one of several thicknesses. This methodology does not appear to have potential, other than for measuring relative oil thickness.

A variety of electrical, optical, and acoustic techniques for measuring oil thickness have been investigated (Goodman et al., 1997; Reimer and Rossiter, 1987). Two promising techniques were pursued in a series of laboratory measurements. In the first technique, known as "thermal mapping," a laser is used to heat a region of oil and the resultant temperature profiles created over a small region

Table 14-2 Relationship between Oil Thickness and Detection Limits in Remote Sensing Instruments

Author	*Year*	*Oil*	*Number*	*Visible Minimum*	*In UV*	*Invisible Camera*	*In IR*	*In SLAR*	*In Microwave*
Congress	1930	Various fuels & bunker	>15	*0.1*					
Horstein	1972	Arab & Louisiana crudes	>20	*<0.15*					
Hollinger	1973	Diesel, fuel oil, bunker C	8				Microwave threshold = 100 µm		
Parker and Cormack	1979	North Sea & Arab crudes	2	*0.1*			25–30	0.1	
						0.1			
Brown et al.	1995	Crude—Norman Wells	32	*0.094*	0.11	0.15			
		Diesel	25	*0.165*	0.11	0.15			
		Lubricating oil	16	*0.077*	0.11	0.15			
		Hydraulic oil	13	*0.159*	0.11	0.15			
Brown et al.	1998	Crude—Federated and Hondo	5–40				No relationship between IR brightness and thickness		
			Average	***0.09***	*0.11*	*0.14*	*25–30*	*0.1*	

near this heating are examined using an infrared camera (Aussel and Monchalin, 1989). The temperature profiles created are dependent on the oil thickness.

Thickness sensors are still in the developmental stages, and it would be premature to use their information for forensic purposes at this time.

A more promising technique involves laser acoustics (Brown et al., 1994; Choquet et al., 1993; Krapez and Cielo, 1992). The laser ultrasonic remote sensing of oil thickness (LURSOT) has been developed under contract to the Industrial Materials Institute (IMI) of the National Research Council of Canada in Boucherville, Quebec. Although complete details of the LURSOT system are beyond the scope of this chapter, a brief overview of the system is presented here.

The LURSOT sensor is a three-laser system with one laser coupled to an optical interferometer to accurately measure oil thickness (Brown et al., 1997b, 2001b, 2005b; Choquet et al., 1993). The measurement process is started by the absorption of a powerful infrared carbon-dioxide (CO_2, ~10 µm) laser pulse that creates a thermal pulse in the oil layer. Rapid thermal expansion of the oil occurs near the surface where the laser beam was absorbed. This leads to a step-like rise of the sample surface and creates an acoustic pulse of high frequency and large bandwidth (<15 MHz for oil). The acoustic pulse travels down through the oil layer to the oil–water interface, where it is largely transmitted (~85%) and partially reflected back (up to 15% depending on the oil) to the oil–air interface, where it causes another small displacement of the oil surface.

The amount of time required for the acoustic pulse to travel through the oil and back to the surface again is a function of the thickness of the oil layer and the acoustic velocity (speed of sound) of the oil. The displacement of the oil layer is measured by a second laser probe beam (Nd:YAG, 1064 µm) aimed at the surface. Motion of the surface causes a phase or frequency shift (Doppler shift) in the reflected probe beam. The modulation of the probe beam is subsequently demodulated with an optical interferometer, either a confocal Fabry–Perot interferometer or a photorefractive interferometer (Monchalin, 1986). The absolute oil slick thickness can be determined from the time of propagation of the acoustic wave between the upper and lower surfaces of the oil layer and the knowledge of the speed of sound in oil. The system uses a third laser (cw HeNe laser, 632.8 nm) to monitor the water surface and generate a trigger pulse when the correct surface geometry for measurement exists.

The initial attempt to test the LURSOT system in an airborne environment was not successful for a number of reasons (Brown et al., 1994a, b). In brief, the extreme operating environment provided by a moving platform was radically different from the laboratory setting in which the prototype was first developed. The broad range of temperatures encountered in the aircraft was found to induce optical beam-path differences in the probe laser (Nd:YAG) that were outside acceptable limits. To correct this, a novel laser system was developed and mounted on a zero thermal expansion carbon-epoxy optical breadboard. In addition, system alignment is conducted at the same temperature expected during flight conditions.

A second alignment problem with the probe laser was corrected by replacing certain mirror mounts with stiffer mounts. The intense vibrations experienced in the airborne environment initially led to the removal of the Fabry–Perot interferometer in favor of a photorefractive interferometer for probe-laser frequency demodulation. The photorefractive interferometer was developed by IMI to provide a demodulation device that is insensitive to vibrations. The photorefractive interferometer was, however, found to be sensitive to frequency changes caused by motion of the target relative to the airborne laser source. To compensate for these frequency (Doppler) shifts, an optical frequency compensation device (OFCD) was designed and tested. To use the OFCD on-board an aircraft, a measurement of vertical velocity was needed. This was fulfilled through the development of a vertical velocity sensor (VVS) by the Institute for Aerospace Research at the National Research Council of Canada in Ottawa. The VVS couples a differential global positioning system (DGPS) receiver with an accelerometer in order to provide real-time vertical velocity measurement. The VVS was tested on-board the aircraft and found to operate satisfactorily when isolated mechanically from the floor of the aircraft and filtered appropriately (Brown et al., 1997a, b). Although this system of compensation was encouraging, the inability to make this system operational in real time prevents its use at this time. It was decided to construct a device to measure the instantaneous optical frequency of the returning target laser beam. This device provides a diagnostic as to how well the optical frequency compensation device is working. Finally, a decision was made to revert to the Fabry–Perot system with enhanced vibrational and acoustic shielding.

There were also concerns about maintaining the colinearity of the three laser beams used in the LURSOT system during flight. A thorough theoretical analysis of the support structure that houses the optical and laser components was undertaken at the University of Toronto's Aerospace Institute in order to understand the effect of vibrations on the colinearity of the optical system. The investigation uncovered several shortcomings with the existing structure and provided the information required to design a structure that provides the stability required to ensure colinearity of the laser beams at the operating altitude of 300 ft.

A technique was developed to measure the in-flight colinearity of the three laser beams used in the LURSOT system. A mirror is used to image the three laser beams onto a thin plate of blackened aluminum. The laser beams in turn heat a spot on the aluminum plate and the infrared camera (sensitive in the thermal infrared) captures an image of these "hot" spots. A suitable delay is added so that each beam can be observed sequentially. During testing, a mirror is moved into position to divert the laser beams onto the aluminum plate. The positions of the three beams are subsequently determined through data analysis of the infrared camera images, and beam colinearity/overlap is confirmed. The redesigned LURSOT system was re-assembled at IMI and tested extensively in a laboratory environment to confirm functionality of individual components and the successful measurement of oil-slick thickness.

The LURSOT was mounted, tested, and certified for airborne operation in Environment Canada's DC-3 aircraft. The LURSOT then participated in a series of flights designed to produce the first airborne measurement of oil-slick thickness. Instead of constructing an expensive large-scale outdoor test tank operation for the LURSOT oil-slick measurement flights, a more economical approach was taken. Five industrial waste dumpsters, 8 ft wide by 20 ft long, were placed on the tarmac at the MacDonald-Cartier International Airport in Ottawa, Canada. The dumpsters were lined with two one-piece polyethylene bag liners (8-mil thick) and filled with water to a depth of approximately 6 in. The water in the test tanks was warmed with heaters (Sinking Tank Heaters, Allied Precision Industries Inc.) to prevent the water from freezing during cold spring evenings. The test tanks were covered with polyethylene covers to help retain heat while not being overflown. Waves were made in the test tanks with pieces of lumber 2 in. × 4 in. × 3 ft) suspended by nylon ropes into the water column. The pieces of lumber were weighted down with steel flat-bars screwed to the underside of the 2 × 4s. Using the nylon ropes, the lumber was lifted manually at regular intervals (~1 Hz) to create waves of the approximate period required in the tanks.

The oil used in the airborne slick measurement experiments was Alberta Sweet Mixed Blend (ASMB), a typical western Canadian crude oil. Oil was added to four of the five tanks to provide nominal slick thicknesses of 1, 3, 6, and 12 mm (based on area and volume of oil added). Physical and chemical properties of ASMB can be found on Environment Canada's Oil Properties Database on the Internet (Environment Canada, 2005).

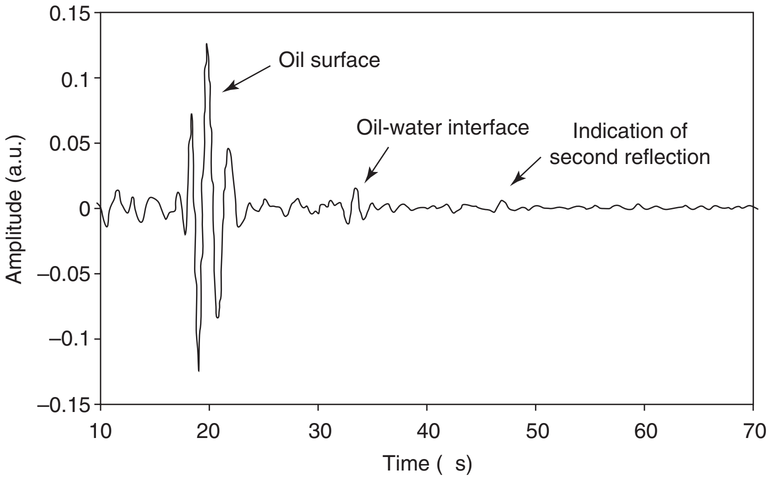

Figure 14-2 The return signals from the LURSOT thickness sensor showing a measurement of 9 mm from a light crude oil. Measurement was taken 61 m above ground with aircraft at 200 km/hr.

These flights were designed to confirm the operation of the triggering mechanism of the LURSOT system. Following the verification of acceptable airborne operation of the individual components of the LURSOT system, a final set of test flights were undertaken to acquire an airborne measurement of oil-slick thickness in the manmade test tanks. Numerous flight lines were flown over the oil-covered test tanks, and the measurement of oil-slick thickness from an airborne platform was successful. A resulting thickness measurement is shown in Figure 14-2.

14.7 Acoustic Systems

Pogorzelski (1995) has shown that acoustic means can be used to measure oil viscosities on the surface. A directional acoustic system employing high-frequency forward specular scattering was used in the laboratory and at sea. Signals scattered are related to the rheological film properties. It is not known at this time if the system is scalable or exactly what the limitations are.

14.8 Satellite Remote Sensing

Optical satellite remote sensing has been used several times to detect oil spills. The slick from the IXTOC I well blowout in Mexico was detected using GOES (Geostationary Operational Environmental Satellite) and by the AVHRR (Advanced Very High Resolution Radiometer) on the LANDSAT satellite (O'Neil et al., 1983). A blowout in the Persian Gulf was subsequently detected. The massive *Exxon Valdez* slick was detected on SPOT (Satellite pour l'Observation de la Terre) satellite data (Dean et al., 1990). Oiled ice in Gabarus Bay resulting from the *Kurdistan* spill was detected using LANDSAT data (Alfoldi and Prout, 1982; Dawe et al., 1981). Several workers were able to detect the Arabian Gulf War Spill in 1991 (Al-Ghunaim et al., 1992; Al-Hinai et al., 1993; Cross, 1992; Rand et al., 1992). The *Haven* spill near Italy was also monitored by satellite (Cecamore et al., 1992). A spill in the Barents Sea was tracked using an IR band on NOAA 10 (Voloshina and Sochnev, 1992). It is significant to note that, in all these cases, the position of the oil was known and data had to be processed to actually see the oil, which usually took several weeks.

Several problems are associated with relying on satellites for oil spill remote sensing. The first is the timing and frequency of overpasses (Clark, 1989) and the absolute need for clear skies to perform optical work.

The chances of the overpass and the clear skies occurring at the same time give a very low probability of seeing a spill on a satellite image. This point is well illustrated in the case of the *Exxon Valdez* spill (Noerager and Goodman, 1991). Although the spill covered vast amounts of ocean for over a month, there was only one clear day that coincided with a satellite overpass, and that was on April 7, 1989. Another disadvantage of satellite remote sensing is the difficulty in developing algorithms to highlight the oil slicks and the long time required to do so. With the *Exxon Valdez* spill, it took more than 2 months before the first group managed to "see" the oil slick in the satellite imagery, although its location was precisely known.

In its present state, optical satellite imagery does not offer much potential for oil spill remote sensing. Radar satellites, including ERS-1 and -2, Radarsat, and ENVISAT, are useful for detecting large offshore spills and for spotting anomalies (Brown et al., 2002c). Radarsat has been used for detecting oil seeps (Biegert et al., 1997) and smaller spills resulting from an oil barge (Werle et al., 1997), although the relative location of these smaller slicks was known before the detection. A novel application of Radarsat has been the study of oil lakes in the deserts of Kuwait (Kwarteng et al., 1997). Radar satellites are now used routinely by a number of nations to provide imagery for larger spills and to give indications of ship discharges. ERS-1 and -2 have been used for mapping of oil spills in the Caspian Sea (Ivanov and Ermoshkin, 2004). Fortuny et al. (2004) describe the use of ERS-2 and ENVISAT to provide imagery during the *Prestige* incident off the coast of Spain.

Several "automatic" systems have been designed for slick detection (Solberg and Theophilopoulos, 1997). Limited testing with ERS-1 has shown that many false signals are present in most locations (Bern et al., 1993; Wahl et al., 1993). Extensive efforts on data processing appear to improve the chances of oil detection (Yan and Clemente-Colon, 1997).

There are problems with resolution and timeliness with all satellite data. A comparison of the use of satellite- versus airborne-derived data showed that satellite data lack resolution and timeliness for many oil spill applications (Fingas and Brown, 1997). It is not clear at this time whether satellite systems can provide any information that is useful for forensic purposes.

14.9 Detection of Oil under Ice

The difficulties in detecting oil in or under ice are numerous (Fingas and Brown, 2002b; Bryce, 2000; Dickins, 2000). Ice is never a homogeneous material but rather it incorporates air, sediment, salt, and water, many of which may present false oil-in-ice signals to the detection mechanisms. In addition, snow on top of the ice or even incorporated into the ice adds further complications. During freeze-up and thaw in the spring, there may not be distinct layers of water and ice. There are many different types of ice and different ice crystalline orientations, which complicate the situation for any potential use in forensics.

The feasibility of various technologies for detecting oil in ice was extensively reviewed by Gill (1979). Based on this feasibility study, some of the technologies were tried on oil under ice in a test tank (Remotec Applications Ltd., 1981; Stapleton et al., 1981). This led to the pursuit of acoustic technologies, which were taken as far as the field testing of a prototype. Many of the other technologies have not been tried since. Much of the literature on the topic is now two decades old.

The acoustical properties of ice are variable (Fingas and Brown, 2002b). Experimenters found that standard acoustic units designed for metal and concrete inspection could be used for oil-in-ice detection (Remotec Applications Ltd., 1981; Stapleton et al., 1981). Initially, this was a surprise because the attenuation of ice and the source of the reflected signal for oil were not readily apparent from the data. Subsequent studies have shown that the physics of sound–oil interaction is relatively simple. There are two sources of signal from oil in or under ice. First, oil reflects the standard compressive (p) wave, and this signal is received by standard acoustic units just like the interfaces in metal or other building materials. But oil behaves acoustically like a non-Newtonian fluid and will also reflect the shear or (s) wave (also called the transverse wave). The s-waves travel at about half the velocity of the compressive waves and could be distinguished by their time delay. One could develop a more discriminating oil-in-ice detector by developing a unit that selectively detected shear waves. In theory, only sediment would propagate similar shear waves.

Jones and Kwan (1982, 1983) and Jones et al. (1984, 1986) developed a detection device consisting of a phased array detector that was capable of detecting shear waves directly and thus determining whether oil was present, with a high factor of reliability. Knudsen Engineering Ltd. (1984) studied the acoustic and electric properties of transducers and the coupling to ice. Goodman et al. (1985a) reviewed the technology and noted the differences in using low- and high-acoustic frequency, the latter yielding better spatial resolution, but with lower penetration capability.

Ice has variable transparency to radiowaves (Fingas and Brown, 2000c). Freshwater ice is relatively transparent, whereas saline first-year ice is highly attenuating. Low frequencies (less than 1 MHz) are best suited to the task of penetrating ice. An important facet of radiofrequency is the dielectric constants of oil, ice, and water. Oil has a dielectric constant of 2 to 3, snow of 1 to 2, and seawater of about 80 (Gill, 1979). Multiyear ice has a dielectric constant of about 3, and first-year ice of 3 to about 5. This differential in dielectric constants has led many theorists to predict that oil should be detectable in ice because of the phase reversals that should be apparent when a wave passes through a dielectric constant of 2 (oil) and immediately hits the seawater with a dielectric constant of 80. If the oil was not there, the dielectric constant would slowly change from that of ice (2 to 5) to that of seawater. This should produce a return due to the strong reflection caused by the dielectric change.

Four types of signal return might be used to detect the presence of oil under ice: (1) out-of-phase returns due to the low conductivity of oil; (2) large amplitude returns due to constructive interference effects; (3) spatial dependence of amplitude-of-return signals due to interference effects; and (4) conductivity differences (Goodman and Fingas, 1983).

Resonance scattering theory was proposed as a means of explaining the signals that might be achieved from plane dielectric layers of oil and ice (Jackins et al., 1982; Dean, 1983; Goodman et al., 1985b). Subsequent analysis by Tunaley (1985), Tunaley and Moorcroft (1986), and MacDougall and Tunaley (1986) showed this to be an inappropriate model. Moorcroft and Tunaley (1985) summarize this in calculations that show there would be essentially no electromagnetic resonance effect in sea ice at frequencies above about 0.2 GHz. This is because of the combined effects of absorption in the conducting sea ice and variations in its thickness. Additional effects are present that serve to eliminate resonances, including scattering of the electromagnetic wave by small-scale surface structure. As a result, there is no possibility of using resonances to detect the presence of oil under sea ice, confirming the findings from the tank experiments.

Several early workers proposed that the oil–ice boundary should be seen in impulse radar outputs (Gill, 1979). Tests during a field test in the Beaufort Sea showed anomalies in the output when the oil and gas were located under the ice (Butt et al., 1981). In another field test, an anomaly was observed in a field test where oil was present (Goobie et al., 1981). The interface was not seen, however, in subsequent tank tests (Remotec Applications Ltd., 1981).

The technology for detecting oil in or under ice is still evolving. Of the many potential technologies reviewed, only acoustic techniques have potential and have been successfully tested in the field. The potential radiofrequency techniques are still awaiting testing in the field or in test tanks. Their use for forensic purposes is still far into the future.

14.10 Real-Time Displays and Printers

The production of data that can be quickly and directly used by operations people is a very important aspect of remote sensing. For forensic applications, the data must also be secure and time-location-stamped in order to be presentable. Real-time displays are important so that remote sensor operators can adjust instruments directly in flight and provide information quickly on the location or state of the spill.

A major concern of the client is that data be rapidly available (Goodman, 1994b). An additional concern is that the data from various sensors be available in a combined or fused form (Zielinski and Robbe, 2004). There is also a need to correct this data for aircraft motion and to annotate the data with time and position. At this time, existing hardware and software must be adapted, as commercial off-the-shelf equipment for directly outputting and printing sensor data is not yet available.

14.11 Future Trends

Advances in sensor technology will continue to influence the use of remote sensors as operational oil spill forensic tools in the future. In the next decade, advances in solid-state laser technology, in particular diode-pumped solid-state lasers, will greatly reduce the size and energy consumption of laser-based remote sensors. This will promote the use of these sensors in smaller, more economical aircraft that are within the budget of many more regulatory agencies and maritime countries. Rapidly improving computer capabilities will allow for true real-time processing. At the present time and for the foreseeable future, there is no single "magic bullet" sensor that will provide all the information required to detect, classify, and quantify oil in the marine and coastal environment for forensic purposes. The laser fluorosensor is currently the only sensor that provides significant forensic benefit.

Recommendations are based on the above considerations and include economy as a major factor. Table 14-3 shows the considerations related to the state of development, cost, and use of the sensor. Table 14-4 shows the suitability of the sensor to various types of missions. The laser fluorosensor offers the only potential for discriminating between oiled and unoiled weeds or shoreline and for positively identifying oil pollution on ice, among ice, and in a variety of other situations. This sensor provides the best potential for forensic use at this time. Most other sensors are experimental or do not offer good potential for forensic applications.

Table 14-3 Attributes for Sensor Selection

Sensor	*State of Development*	*Amount of Experience in Use*	*Specific to Oil*	*Immunity to False Targets*	*Forensic Application*	*Acquisition Cost Range (k$)*	*Aircraft Physical Requirements*
Still camera—Film	High	High	Poor	Poor	Documentation	0.25 to 5	No
Still camera—CCD	High	High	Poor	Poor	Documentation	1 to 20	No
Video	High	High	Poor	Poor	Documentation	1 to 10	No
IR camera (3 to 5 μm)	High	Medium	Poor	Poor	Documentation	4 to 20	No
IR camera (8 to 14 μm)	Medium	Medium	Medium	Medium	Documentation	20 to 200	No
UV camera	Medium	Medium	Poor	Poor	Documentation	4 to 20	No
Multi-spectral scanner	Medium	Medium	Poor	Poor	Documentation	100 to 300	Some
Radar	High	High	Medium	Poor	Little	1200 to 8000	Yes—Dedicated
Microwave radiometer	Medium	Medium	Medium	Medium	Very little	400 to 2000	Yes—Dedicated
Laser fluorosensor	Medium	Limited	Good	Good	Good	300 to 2000	Yes—Dedicated

Table 14-4 Sensor Suitability for Various Missions

Sensor	*Support for Cleanup*	*Night and Fog Operation*	*Detection of Oil with Debris*	*Oiled Shoreline Survey*	*Spill Mapping*	*Ship Discharge Surveillance*	*Enforcement and Prosecution*
Still camera—film	n/a	n/a	n/a	1	1	3	3
Still camera—CCD	2	n/a	1	2	2	2	2
Video	2	n/a	1	2	2	2	2
IR camera (3 to 5 µm)	3	2	1	n/a	3	2	2
IR camera (8 to 14 µm)	4	2	1	n/a	3	3	3
UV camera	2	n/a	n/a	n/a	3	2	1
UV/IR scanner	4	2	1	n/a	4	3	3
Multi-spectral scanner	1	n/a	n/a	1	2	1	1
Radar	n/a	4	n/a	n/a	4	3	2
Microwave radiometer	1	3	n/a	n/a	2	2	1
Laser fluorosensor	4	3	5	5	1	5	5

Key: n/a = not applicable; numerical values represent a scale from 1 = poorly suited to 5 = ideally suited.

References

Al-Ghunaim, I., M. Abuzar, and F.S. Al-Qurnas, Delineation and monitoring of oil spill in the Arabian Gulf using Landsat thematic mapper (TM) data. In *Proc. First Thematic Conf. Remote Sensing for Marine and Coastal Environ*. ERIM Conferences, Ann Arbor, MI, 1992, 1151–1160.

Al-Hinai, K.G., M.A. Khan, A.E. Dabbagh, and T.A. Bader, Analysis of Landsat thematic mapper data for mapping oil slick concentrations — Arabian Gulf oil spill 1991. *The Arabian J. Sci. Eng.*, 1993, **18**(2), 85–93.

Alfoldi, T.T. and N.A. Prout, The use of satellite data for monitoring oil spills in Canada Environment Canada Report EPS 3-EC-82-5, Ottawa, ON, 1982.

Allen, A.A. and R.S. Schlueter, Estimates of surface pollution resulting from submarine oil seeps at platform A and coal oil point. General Research Corp., prepared for Santa Barbara County, Santa Barbara, CA, 1969.

Allen, A.A. and R.S. Schlueter, Natural oil seepage at Coal Oil Point, Santa Barbara, California. *Science*, 1970, **170**, 974–977.

Anderson, S.G., Dual laser system provides real-time fluorescence images. *Laser Focus World*, 1994, **August**, 15.

API, *Manual on Disposal of Refinery Wastes, Volume on Liquid Wastes*, American Petroleum Institute, 1969.

Aussel, J.D. and J.-P. Monchalin, Laser-ultrasonic measurement of oil thickness on water from aircraft, feasibility study. Industrial Materials Research Institute Report, Boucherville, Quebec, Canada, 1989.

Bagheri, S., M. Stein, and C. Zetlin, Utility of airborne videography as an oil spill-response monitoring system. In *Encyclopedia of Environ. Control Tech.*, Houston, TX: Gulf Publishing Company, 1995, 367–376.

Balick, L., J.A. DiBenedetto, and S.S. Lutz, Fluorescence emission spectral measurements for the detection of oil on shore. In *Proc. Fourth Thematic Conf. Remote Sensing for Marine and Coastal Environ*. Ann Arbor, MI: Environmental Research Institute of Michigan, 1997, **I**, 13–20.

Barbini, R., R. Fantoni, A. Palucci, S. Ribezzo, and H.J.L. Van der Steen, Fluorosensor lidar for environmental diagnostics. In *Proc. Conf. — Quantum Electronics and Plasma Physics*, Bologna: SIF, 1991, **29**, 383–387.

Bartsch, N., K. Grüner, W. Keydel, and F. Witte, Contribution to oil spill detection and analysis with radar and microwave radiometer: Results of the Archimedes II campaign. *IEEE Trans. Geosci. Remote Sensing*, 1987, **GE.25**(6), 677–690.

Belore, R.C., A device for measuring oil slick thickness. *Spill Tech. Newsletter*, 1982, **7**(2), 44–47.

Bern, T-I., T. Wahl, T. Anderssen, and R. Olsen, Oil spill detection using satellite-based SAR: Experience from a field experiment. *Photogrammetric Eng. Remote Sensing*, 1993, **59**(3), 423–428.

Bianchi, R., R.M. Cavalli, C.M. Marino, S. Pignatti, and M. Poscolieri, Use of airborne hyperspectral images to assess the spatial distribution of oil spilled during the Trecate blow-out (Northern Italy). *SPIE*, 1995, **2585**, 352–362.

Biegert, E.K., R.N. Baker, J.L. Berry, S. Mott, and S. Scantland, Gulf offshore satellite applications project detects oil slicks using Radarsat. In *Proc. Intl. Symp. Geomatics in the Era of Radarsat*, Ottawa, Ontario, Canada, 1997.

Bolus, R.L., Airborne testing of a suite of remote sensors for oil spill detecting on water. In *Proc. Second Thematic Intl. Airborne Remote Sensing Conf. Exhibition*, Ann Arbor, MI: Environmental Research Institute of Michigan, 1996, III-743–III-752.

Brown, C.E. and M.F. Fingas, Review of the development of laser fluorosensors for oil spill application. *Mar. Poll. Bull.*, 2003, **47**, 477–484.

Brown, C.E., M. Fruhwirth, M.F. Fingas, R.H. Goodman, M. Choquet, R. Héon, G. Vaudreuil, J.-P. Monchalin, and C. Padioleau, Laser ultrasonic remote sensing of oil thickness: Absolute measurement of oil slick thickness. In *Proc. First Intl. Airborne Remote Sensing Conf. Exhibition*, Ann Arbor, MI: Environmental Research Institute of Michigan, 1994, **1**, I-567–I-578.

Brown, C.E., M. Fruhwirth, Z. Wang, P. Lambert, and M. Fingas, Airborne oil spill sensor test program. In *Proc. Second Thematic Conf. Remote Sensing for Mar. Coastal Environ.: Needs, Solutions and Applic.*, Ann Arbor, MI: ERIM Conferences, 1994a, I-19–33.

Brown, C.E., Z. Wang, M. Fruhwirth, and M. Fingas, May 1993 oil-spill sensor test program: Correlation of laser fluorosensor data with chemical analysis. In *Proc. Seventeenth Arctic and Marine Oilspill Tech. Sem.*, Ottawa, Ontario: Environment Canada, 1994b, 1239–1261.

Brown, C.E., M. Fruhwirth, R. Nelson, and M.F. Fingas, Real-time response with a laser fluorosensor: The integration of fluorescence data with down-looking video images and the prompt delivery of hard-copy maps. In *Proc. Second Intl. Airborne Remote Sensing Conf. Exhibition*, Ann Arbor, MI: ERIM Conferences, 1996, III-673–681.

Brown, C.E., R. Nelson, M.F. Fingas, and J.V. Mullin, Airborne laser fluorosensing: Overflights during lift operations of a sunken oil barge. In *Proc. Fourth Thematic Conf. Remote Sensing for Mar. Coastal Environ.*, Ann Arbor, MI: Environmental Research Institute of Michigan, 1997a, **I**, 23–30.

Brown, C.E., M.F. Fingas, R.H. Goodman, M. Choquet, A. Blouin, D. Drolet, J.-P. Monchalin, and C.D. Hardwick, The LURSOT sensor: Providing absolute measurements of oil slick thickness. In *Proc. Fourth Thematic Conf. Remote Sensing for Mar. Coastal Environ.*, Ann Arbor, MI: Environmental Research Institute of Michigan, 1997b, **I**, 393–397.

Brown, C.E., R. Marois, M.F. Fingas, and J.V. Mullin, Preliminary testing of the scanning laser environmental airborne fluorosensor. In *Proc. Twenty-Third Arctic and Mar. Oilspill Program Techn. Sem.*, Ottawa, ON: Environment Canada, 2000a, 519–523.

Brown, C.E., M.F. Fingas, and J. An, Laser fluorosensors: A survey of applications and developments of a versatile sensor. In *Proc. Twenty-Fourth Arctic and Mar. Oilspill Program Tech. Sem.*, Ottawa, ON: Environment Canada, 2001a, 485–493.

Brown, C.E., R. Marois, M.F. Fingas, M. Choquet, J-P. Monchalin, J. Mullin, and R. Goodman, Airborne oil spill sensor testing: Progress and recent developments. In *Proc. 2001 Intl. Oil Spill Conf.*, Washington, DC: American Petroleum Institute, 2001b, 917–921.

Brown, C.E., M.F. Fingas, R.M. Gamble, and A.E. Myslicki, The remote detection of submerged oil. In *Proc. Third R&D Forum on High-Density Oil Spill Response*. London: International Maritime Organization, 2002a, 46–54.

Brown, C.E., R. Marois, G. Myslicki, and M.F. Fingas, Initial studies on the remote detection of submerged orimulsion with a range-gated laser fluorosensor. In *Proc. Twenty-Fifth Arctic and Marine Oilspill Program Tech. Sem.*, Ottawa, ON: Environment Canada, 2002b, 773–783.

Brown, C.E., M.F. Fingas, and T.J. Lukowski, Airborne and space-borne synergies: The old dog teaches tricks to a new bird. In *Proc. Fifth Intl. Airborne Remote Sensing Conf. Exhibition*, Ann Arbor, MI: Veridien, 2002c, 8.

Brown, C.E., R. Marois, R.M. Gamble, and M.F. Fingas, Further studies on the remote detection of submerged orimulsion with a range-gated laser fluorosensor. In *Proc. Twenty-Sixth Arctic and Marine Oilspill Program Tech. Sem.*, Ottawa, ON: Environment Canada, 2003a, 279–286.

Brown, C.E., R. Marois, G. Myslicki, M.F. Fingas, and R. MacKay, Remote detection of submerged orimulsion with a range-gated laser fluorosensor. In *Proc. 2003 Intl. Oil Spill Conf.*, Washington, DC: American Petroleum Institute, 2003b, 779–784.

Brown, C.E., M.F. Fingas, and R. Marois, Oil spill remote sensing: Laser fluorosensor demonstration flights off the east coast of Canada. In *Proc. Twenty-Seventh Arctic and Marine Oilspill Program Tech. Sem.*, Ottawa, ON: Environment Canada, 2004a, 317–334.

Brown, C.E., M. Fingas, R. Marois, B. Fieldhouse, and R.L. Gamble, Remote sensing of water-in-oil emulsions: Initial laser fluorosensor studies. In *Proc. Twenty-Seventh Arctic and Marine Oilspill Program Tech. Sem.*, Ottawa, ON: Environment Canada, 2004b, 295–316.

Brown, C.E., M.F. Fingas, and R. Marois, Oil spill remote sensing flights in the coastal waters around newfoundland. In *Proc. Eighth Intl. Conf. Remote Sensing for Marine and Coastal Environ.*, Ann Arbor, MI, 2005a, 8.

Brown, C.E., M.F. Fingas, J-P. Monchalin, C. Neron, and C. Padioleau, Airborne oil slick thickness measurements: Realization of a dream. In *Proc. Eighth Intl. Conf. Remote Sensing for Marine and Coastal Environ.*, Ann Arbor, MI: Altarum, 2005b, 8.

Brown, H.M. and Goodman, R.H. In-situ burning of oil in ice leads. In *Proc. Ninth Annual Arctic and Marine Oilspill Program Tech. Sem.*, Ottawa, ON: Environment Canada, 1986, 245–256.

Brown, H.M., J.P. Bittner, and R.H. Goodman, Visibility limits of spilled oil sheens. Imperial Oil Internal Report, Calgary, AB, 1995.

Brown, H.M., J.P. Bittner, and R.H. Goodman, The limits of visibility of spilled oil sheens. In *Proc. Second Thematic Intl. Airborne Remote Sensing Conf. Exhibition*, Ann Arbor, MI: Environmental Research Institute of Michigan, 1996, III-327–III-334.

Brown, H.M., J.J. Baschuk, and R.H. Goodman, The limits of visibility of spilled oil sheens. In *Proc. Twenty-First Arctic and Marine Oilspill Program Tech. Sem.*, Ottawa, ON: Environment Canada, 1998, 805–810.

Bryce, P., Design considerations for Arctic subsea leak detection systems. In *Proc. Intl. Oil and Ice Workshop*, Anchorage, AK: ACS, 2000.

Butt, K., P. O'Reilly, and E. Reimer, A field evaluation of impulse radar for detecting oil in and under sea ice. *Oil and Gas Under Sea Ice Experiment*, Dome Petroleum, APOA Contract 169, 1981.

Calleri, F. and P.L. Bernardi, Airborne fluorescence lidar system. In *Proc. Intl. Symp. Operationalization of Remote Sensing*, Enschede: ITC, 1993, **17**, 87–97.

Canadian Coast Guard, Appearance and thickness of an oil slick. *Operations Manual*, Section 3, Annex C, Ottawa, ON, 1996.

Castagnoli, F., G. Cecchi, L. Pantani, I. Pippi, B. Radicati, and P. Mazzinghi, A fluorescence LIDAR for land and sea remote sensing. *SPIE*, **663**, *Laser Radar Techn. Applic.*, 1986, 212–216.

C-CORE (Centre for Cold Ocean Resources Engineering), Microwave systems for detecting oil slicks in ice-infested waters: Phase I — literature review and feasibility study, Environment Canada Report EPS 3-EC-81-3, Ottawa, ON, 1981, 353.

Cecamore, P., A. Ciappa, and V. Perusini, Monitoring the oil spill following the wreck of the tanker *HAVEN* in the Gulf of Genoa through satellite remote sensing techniques. In *Proc. First Thematic Conf. Remote Sensing for Marine and Coastal Environ.*, Ann Arbor, MI: ERIM Conferences, 1992, 183–189.

Choquet, M., R. Héon, G. Vaudreuil, J.-P. Monchalin, C. Padioleau, and R.H. Goodman, Remote thickness measurement of oil slicks on water by laser ultrasonics. In *Proc. 1993 Intl. Oil Spill Conf.*, Washington, DC: American Petroleum Institute, 1993, 531–536.

Clark, C.D., Satellite remote sensing for marine pollution investigations. *Mar. Poll. Bull.*, 1989, **26**(7), 92–96.

Congress, Report on oil-pollution experiments — behaviour of fuel oil on the surface of the sea. Hearings before the Committee on River and Harbors, 71st Congress, 2nd Session, H.R. 10625, Part I, 41–9, Washington, DC, May 2, 3, and 26, 1930.

Cross, A., Monitoring marine oil pollution using AVHRR data: Observations off the Coast of Kuwait and Saudi Arabia during January 1991. *Intl. J. Remote Sensing*, 1992, **13**, 781–788.

Dawe, B.R., S.K. Parashar, T.P. Ryan, and R.O. Worsfold, The use of satellite imagery for tracking the *Kurdistan* oil spill. Environment Canada Report EPS 4-EC-81-6, Ottawa, ON, 1981, 31.

Dean, A.M., Investigating the practical applications of the resonant scattering theory for the detection of oil under sea ice. In *Proc. Sixth Annual Arctic Marine Oilspill Program Tech. Sem.*, Ottawa, ON: Environment Canada, 1983, 235–260.

Dean, K.G., W.J. Stringer, J.E. Groves, K. Ahlinas, and T.C. Royer, The *Exxon Valdez* oil spill: Satellite analyses. In *Oil Spills: Management and Legislative Implications*, M.L. Spaulding and M.

Reed (eds.), New York: American Society of Civil Engineers, 1990, 492–502.

Dick, R., M. Fruhwirth, M.F. Fingas, and C.E. Brown, Laser fluorosensor work in Canada. In *Proc. First Thematic Conf.: Remote Sensing for Marine and Coastal Environ*., Ann Arbor, MI: Environmental Research Institute of Michigan, 1992, 223–236.

Dickins, D.F., Detection and tracking of oil under ice. In *U.S. Minerals Mgt. Report*, Herndon, VA, 2000.

Diebel, D., T. Hengstermann, R. Reuter, and R. Willkomm, Laser fluorosensing of mineral oil spirits. In *The Remote Sensing of Oil Slicks*, A.E. Lodge (ed.), Chichester, UK: John Wiley and Sons, 1989, 127–142.

Duckworth, R., unpublished data report in MacDonald et al., 1993.

Dyring, A. and O. Fäst, MSS puts the aircraft in the oil spill tracking network. In *Proc. Interspill*, Trondheim, Norway, 2004.

Environment Canada, Oil properties database, http://www.etc-cte.ec.gc.ca/databases/OilProperties/Default.aspx, 2005.

Fäst, O., Remote sensing of oil on water — air and space-borne systems. In *Proc. DOOS Sem.*, SINTEF, Trondheim, Norway, 1986.

Fingas, M.F., A simple night time oil slick detector. *Spill Tech. Newsletter*, 1982, **7**(1), 137–141.

Fingas, M.F. and C.E. Brown, Airborne oil spill remote sensors — do they have a future? In *Proc. Third Intl. Airborne Remote Sensing Conf. Exhibition*, Ann Arbor, MI: Environmental Research Institute of Michigan, 1997, 715–722.

Fingas, M.F. and C.E. Brown, Review of oil spill remote sensing. In *Proc. Fifth Intl. Conf. Remote Sensing for Marine and Coastal Environ*., Ann Arbor, MI: Environmental Research Institute of Michigan (ERIM), 2000a, I211–218.

Fingas, M.F. and C.E. Brown, Review of oil spill remote sensing. In *Proc. SPILLCON 2000*, Australian Marine Safety Authority, Sydney, Australia, www.meetingplanners.com.au/spillcon/, 2000b.

Fingas, M.F. and C.E. Brown, A review of the status of advanced technologies for the detection of oil in and with ice. *Spill Sci. Tech. Bull.*, 2000c, **6**(5/6), 295–302.

Fingas, M.F. and C.E. Brown, Review of oil spill remote sensors. In *Proc. Seventh Intl. Conf. Remote Sensing for Marine and Coastal Environ*., Ann Arbor, MI: Veridien, 2002a, 9.

Fingas, M.F. and C.E. Brown, Detection of oil in and under ice. In *Proc. Twenty-Fifth Arctic and Marine Oilspill Program Tech. Sem.*, Ottawa, ON: Environment Canada, 2002b, 199–214.

Fingas, M.F. and C.E. Brown, An update on oil spill remote sensors. In *Proc. Twenty-Eighth Arctic and Marine Oilspill Program Tech. Sem.*, Ottawa, ON: Environment Canada, 2005, 825–860.

Fingas, M.F., C.E. Brown, and L. Gamble, The visibility and detectability of oil slicks and oil discharges on water. In *Proc. Twenty-Second Arctic and Marine Oilspill Program Tech. Sem.*, Ottawa, ON: Environment Canada, 1999, 865–886.

Forget, P. and P. Brochu, Slicks, waves and fronts observed in sea coastal area by an X-band airborne synthetic aperture radar. *Remote Sensing of the Environ.*, 1996, **57**, 1–12.

Fortuny, J., D. Tarchi, G. Ferraro, and A. Sieber, The use of satellite radar imagery in the prestige accident. In *Proc. Interspill*, Trondheim, Norway, 2004.

Frysinger, G.S., W.E. Asher, G.M. Korenowski, W.R. Barger, M.A. Klusty, N.M. Frew, and R.K. Nelson, Study of ocean slicks by nonlinear laser processes in second-harmonic generation. *J. Geophys. Res*., 1992, **97**(C4), 5253–5269.

Gade, M., W. Alpers, H. Hüehnerfuss, and V. Wismann, Radar signatures of different oceanic surface films measured during the SIR-C-X-SAR missions. *Remote Sensing (96)*, 16th Symp. Eur. Associ. of Remote Sensing Lab. (EARsel), Rotterdam, Holland, 1996, 233–240.

Gangeskar, R., Automatic oil-spill detection by marine X-band radars. *Sea Tech.*, 2004, **Aug**, 40–45.

Geraci, A.L., F. Landolina, L. Pantani, and G. Cecchi, Laser and infrared techniques for water pollution control. In *Proc. 1993 Oil Spill Conf.*, Washington, DC: American Petroleum Institute, 1993, 525–529.

Gill, R., Feasibility of surface detection of oil under ice. Environ. Protection Service Report EPS 3-EC-79-11, Environment Canada, Ottawa, ON, 1979.

Goobie, G.I., T.W. Laidley, and E.M. Reimer, C-CORE oil spill research activities. In *Proc. Fourth Annual Arctic Marine Oilspill Program Tech. Sem.*, Ottawa, ON: Environment Canada, 1981, 623–643.

Goodman, R.H., Simple remote sensing system for the detection of oil on water. Environmental Studies Research Fund Report Number 98, Ottawa, ON, 1988, 31.

Goodman, R.H., Application of the technology in North America. In *The Remote Sensing of Oil Slicks*, A.E. Lodge (ed.), Chichester, UK: John Wiley and Sons, 1989, 39–65.

Goodman, R.H., Remote sensing resolution and oil slick inhomogeneities. In *Proc. Second Thematic Conf. Remote Sensing for Marine and Coastal Environ.: Needs, Solutions and Applica.*, Ann Arbor, MI: ERIM Conferences, 1994a, I-1–17.

Goodman, R.H., Overview and future trends in oil spill remote sensing. *Spill Sci. Tech.*, 1994b, **1**(1), 11–21.

Goodman, R.H. and M.F. Fingas, Detection of oil-under-ice — a joint Esso/EPS project. In *Proc. Sixth Annual Arctic Marine Oilspill Program Tech. Sem.*, Ottawa, ON: Environment Canada, 1983, 207–214.

Goodman, R.H. and M.F. Fingas, The use of remote sensing for the determination of dispersant effectiveness. In *Proc. Eleventh Arctic and Marine Oilspill Program Tech. Sem.*, Ottawa, ON: Environment Canada, 1988, 377–384.

Goodman, R.H., H. Jones, and M.F. Fingas, The detection of oil under ice using acoustics. In *Proc. Conf. Port and Ocean Eng. under Arctic Conditions*, 1985a, 903–916.

Goodman, R.H., A. Dean, and M.F. Fingas, The detection of oil under ice using electromagnetic radiation. In *Proc. Conf. Port and Ocean Eng. under Arctic Conditions*, 1985b, 895–902.

Goodman, R., H. Brown, and J. Bittner, The measurement of thickness of oil on water. In *Proc. Fourth Thematic Conf. Remote Sensing for Marine and Coastal Environ.*, Ann Arbor, MI: Environmental Research Institute of Michigan, 1997, **I**, 31–41.

Gruner, K., R. Reuter, and H. Smid, A new sensor system for airborne measurements of maritime pollution and of hydrographic parameters. *GeoJournal*, 1991, **24**(1), 103–117.

Hengstermann, T. and R. Reuter, Lidar fluorosensing of mineral oil spills on the sea surface. *Appl. Opt.*, 1990, **29**, 3218–3227.

Hielm, J.H., NIFO comparative trials. In *The Remote Sensing of Oil Slicks*, A.E. Lodge (ed.), Chichester, UK: John Wiley and Sons, 1989, 67–75.

Hoge, F.E. and R.N. Swift, Oil film thickness measurement using airborne laser-induced water Raman backscatter. *Appl. Opt.*, 1980, **19**(19), 3269–3281.

Hollinger, J.P. and R.A. Mennella, Oil spills: Measurements of their distributions and volumes by multifrequency microwave radiometry. *Science*, 1973, **181**, 54–56.

Horstein, B., The appearance and visibility of thin oil films on water. Environmental Protection Agency Report, EPA-R2-72-039, Cincinnati, OH, 1972.

Horstein, B., The visibility of oil-water discharges. In *Proc. 1973 Intl. Oil Spill Conf.*, Washington, DC: American Petroleum Institute, 1973, 91–99.

Hover, G.L., Testing of infrared sensors for U.S. Coast Guard oil spill response applications. In *Proc. Second Thematic Conf. Remote Sensing for Marine and Coastal Environ.: Needs, Solutions and Applications*, ERIM Conferences, Ann Arbor, MI, 1994, I-47–58.

Hover, G.L. and J.V. Plourde, Evaluation of night capable sensors for the detection of oil on water. USCG Report Number CG-D-009-94, available as NTIS Report Number ADA281728, 1994.

Hühnerfuss, H., W. Alpers, and F. Witte, Layers of different thicknesses in mineral oil spills detected by grey level textures of real aperture radar images. *Intol. J. Remote Sensing*, 1989, **10**, 1093–1099.

Hühnerfuss, H., W. Alpers, H. Dannhauer, M. Gade, P.A. Lange, V. Neumann, and V. Wismann, Natural and man-made sea slicks in the North Sea investigated by a helicopter-borne 5-frequency radar scatterometer. *Int. J. Remote Sensing*, 1996, **17**(8), 1567–1582.

Hurford, N., Review of remote sensing technology. In *The Remote Sensing of Oil Slicks*, A.E. Lodge (ed.), Chichester, UK: John Wiley and Sons, 1989, 7–16.

Hurford, N. and F.N. Martinelli, Use of an infrared line scanner and a side-looking airborne radar to detect oil discharges from ships. Warren Spring Laboratory Report, Stevenage, UK, 1982.

Hurford, N. and F.N. Martinelli, Use of an infrared line scanner and a side-looking airborne radar to detect oil discharges from ships. In *Remote Sensing for the Control of Marine Poll.*, J. M. Massin (ed.), New York: Plenum Press, 1984, 405–421.

Intera Technologies, Radar surveillance in support of the 1983 COATTF oil spill trials. Environment Canada Manuscript Report EE-51, Ottawa, ON, 1984, 48.

ITOPF, Aerial observation of oil at sea. Intl. Tanker Owners Poll. Fed., London, 1981.

Ivanov, A.Y. and I.S. Ermoshkin, Mapping of oil spills in the Caspian Sea using the ERS-1.ERS-2

SAR image quick-looks and GIS. In *Proc. Interspill*, Trondheim, Norway, 2004.

Jackins, P.D., G.C. Gaunaurd, and C.D. McKindra, Radar resonance reflection from sets of plane dielectric layers. In *Proc. Fifth Annual Arctic Marine Oilspill Program Tech. Sem.*, Ottawa, ON: Environment Canada, 1982, 365–390.

James, R.T.B. and R. Dick, Design of algorithms for the real-time airborne detection of littoral oil-spills by laser-induced fluorescence. In *Proc. Nineteenth Arctic and Marine Oilspill Tech. Sem.*, Ottawa, ON: Environment Canada, 1996, 1599–1608.

Jones, H.W. and H.W. Kwan, The detection of oil spills under arctic ice by ultrasound. In *Proc. Fifth Annual Arctic Marine Oilspill Program Tech. Sem.*, Ottawa, ON: Environment Canada, 1982, 391–411.

Jones, H.W. and H.W. Kwan, The detection of oil spills under seawater in the Arctic Ocean. In *Proc. Sixth Annual Arctic Marine Oilspill Program Tech. Sem.*, Ottawa, ON: Environment Canada, 1983, 241–252.

Jones, H.W., H.W. Kwan, and E.M. Yeatman, On the design of an apparatus to detect oil trapped under sea ice. In *Proc. Seventh Annual Arctic Marine Oilspill Program Tech. Sem.*, Ottawa, ON: Environment Canada, 1984, 295–305.

Jones, H.W., H.W. Kwan, T. Hayman, and E.M. Yeatman, The detection of oil under ice by ultrasound using multiple element phased arrays. In *Proc. Ninth Annual Arctic Marine Oilspill Program Tech. Sem.*, Ottawa, ON: Environment Canada, 1986, 475–484.

Kennicutt, M.C., I.R. MacDonald, T. Rogne, C. Giammona, and R. Englehardt, The Tenyo Maru oil spill: A multi-spectral and sea truth experiment. In *Proc. 1992 Arctic and Marine Oilspill Tech. Sem.*, Ottawa, ON: Environment Canada, 1992, 349–356.

Knudsen Engineering Ltd., Experiments in the detection of oil under ice. Environment Canada Manuscript Report, Ottawa, ON, 1984.

Koechler, C., J. Verdebout, G. Bertolini, A. Gallotti, E. Zanzottera, G. Cavalcabo, and L. Fiorina, Determination of aquatic parameters by a time-resolved laser fluorosensor operating from a helicopter. *SPIE*, **1714**, *Lidar for Remote Sensing*, 1992, 93–107.

Kozu, T., T. Umehara, T. Ojima, T. Suitsu, H. Masuyko, and H. Inomata, Observation of oil slicks on the ocean by X-Band SLAR. In *Proc. IGARSS '87 Sym.*, Ann Arbor, MI, 1987, 735–740.

Krapez, J.C. and P. Cielo, Optothermal evaluation of oil film thickness. *J. Appl. Phys.*, 1992, **72**(4), 1255–1261.

Kwarteng, A.Y., V. Singhroy, R. Saint-Jean, and D. Al-Ajmi, Radarsat SAR data assessment of the oil lakes in the Greater Burgan Oil Field, Kuwait. In *Proc. Intl. Symp.: Geomatics in the Era of Radarsat*, Ottawa, ON, 1997.

Lehr, W.J., Oil spill monitoring using a field microcomputer-GPS receiver combination. In *Proc. Second Thematic Conf. Remote Sensing for Marine and Coastal Environ.: Needs, Solutions and Applications*, Ann Arbor, MI: ERIM Conferences, 1994, I-435–439.

MacDonald, I.R., N.L. Guinasso, Jr., S.G. Ackleson, J.F. Amos, R. Duckworth, R. Sassen, and J.M. Brooks, Natural oil slicks in the Gulf of Mexico visible from space. *J. Geophys. Res.*, 1993, **98**(C9), 16351–16364.

MacDougall, J.W. and J.K.E. Tunaley, The complex permittivity of crude oil. In *Proc. Ninth Annual Arctic Marine Oilspill Program Tech. Sem.*, Ottawa, ON: Environment Canada, 1986, 413–420.

Macklin, J.T., The imaging of oil slicks by synthetic aperture radar. *GEC J. Res.*, 1992, **10**(1), 19–28.

Madsen, S., N. Skou, and B.M. Sorensen, Comparison of VV and HH polarized SLAR for detection of oil on the sea surface. In *Proc. Second Thematic Conf. Remote Sensing for Marine and Coastal Environ.: Needs, Solutions and Applications*, Ann Arbor, MI: ERIM Conferences, 1994, I-498–503.

Marmorino, G.O., D.R. Thompson, H.C. Graber, and C.L. Trump, Correlation of oceanographic signatures appearing in synthetic aperture radar and interferometric synthetic aperture radar imagery with in-situ measurements. *J. Geophys. Res.*, 1997, **102**(C8), 18723–18736.

Mastin, G.A., J.J. Mason, J.D. Bradley, R.M. Axline, and G.L. Hover, A comparative evaluation of SAR and SLAR. In *Proc. Second Thematic Conf. Remote Sensing for Marine and Coastal Environ.: Needs, Solutions and Applications*, Ann Arbor, MI: ERIM Conferences, 1994, I-7–17.

McMahon, O.B., E.R. Brown, G.D. Daniels, T.J. Murphy, and G.L. Hover, Oil thickness detection using wideband radiometry. In *Proc. Intl. Oil Spill Conf.*, Washington, DC: American Petroleum Institute, 1995, 15–20.

McMahon, O.B., T.J. Murphy, and E.R. Brown, Remote measurement of oil spill thickness. In *Proc. Fourth Thematic Conf. Remote Sensing for Marine and Coastal Environ*., Ann Arbor, MI: Environmental Research Institute of Michigan, 1997, **1**, 353–360.

Measures, R.M. and M. Bristow, The development of a laser fluorosensor for remote environmental probing. *Can. Aeron. Space J*., 1971, **17**, 421–422.

Monchalin, J.P., Optical detection of ultrasound. *IEEE Transa. Ultrasonics, Ferroelectrics and Frequency Control*, 1986, **UFFC-33**(5), 485–499.

Moorcroft, D.R. and J.K.E. Tunaley, Electromagnetic resonance in layers of sea ice over sea water. In *Proc. Eighth Annual Arctic Marine Oilspill Program Tech. Sem.*, Ottawa, ON: Environment Canada, 1985, 269–277.

Mussetto, M.S., L. Yujiri, D.P. Dixon, B.I. Hauss, and C.D. Eberhard, Passive millimeter wave radiometric sensing of oil spills. In *Proc. Second Thematic Conf. Remote Sensing for Marine and Coastal Environ.: Needs, Solutions and Applications*, Ann Arbor, MI: ERIM Conferences, 1994, I-35–46.

NASA, Airborne oceanographic lidar. http://aol.wff.nasa.gov/html/aoldes.html, 2001.

Neville, R.A., V. Thompson, K. Dagg, and R.A. O'Neil, An analysis of multispectral line scanner imagery from two test spills. In *Proc. First Workshop Sponsored by Working Group I of the Pilot Study on the Use of Remote Sensing for the Control of Marine Poll., NATO Challenges of Modern Society*, 1979, **6**, 201–215.

Noerager, J.A. and R.H. Goodman, Oil tracking, containment and recovery during the *Exxon Valdez* response. In *Proc. 1991 Oil Spill Conf.*, Washington, DC: American Petroleum Institute, 1991, 193–203.

O'Neil, R.A., R.A. Neville, and V. Thompson, The Arctic marine oilspill program (AMOP) remote sensing study. Environment Canada Report EPS 4-EC-83-3, Ottawa, ON, 1983, 257.

Okamoto, K., T. Kobayashi, H. Masuko, S. Ochiai, H. Horie, H. Kumagai, K. Nakamua, and M. Shimada, Results of experiments using synthetic aperture radar onboard the European remote sensing satellite 1–4. Artificial oil pollution detection. *J. Comm. Res. Lab*., 1996, **43**(3), 327–344.

Palmer, D., G.A. Borstad, and S.R. Boxall, Airborne multi spectral remote sensing of the January 1993 Shetlands oil spill. In *Proc. Second Thematic Conf. Remote Sensing for Marine and Coastal Environ.: Needs, Solutions and Applications*, Ann Arbor, MI: ERIM Conferences, 1994, II-546–558.

Pantani, L., G. Cecchi, and M. Bazzani, Remote sensing of marine environments with the high spectral resolution fluorosensor, FLIDAR 3. *SPIE*, 1995, **2586**, 56–64.

Parker, H.D. and D. Cormack, Evaluation of infrared line scan (IRLS) and side-looking airborne radar (SLAR) over controlled oil spills in the North Sea. Warren Spring Laboratory Report, 1979.

Patsayeva, S., V. Yuhakov, V. Varlamov, R. Barbini, R. Fantoni, C. Frassanito, and A. Palucci, Laser spectroscopy of mineral oils on the water surface. In *Proc. Fourth EARSeL Workshop Lidar Remote Sensing of Land and Sea*, http://las.physik.uni-oldenburg.de/projekte/earsel/4th_workshop.html#proceedings, 2000.

Pelyushenko, S.A., Microwave radiometer system for the detection of oil slicks. *Spill Sci. Tech. Bull*., 1995, **2**(4), 249–254.

Pelyushenko, S.A., The use of microwave radiometer scanning system for detecting and identification of oil spills. In *Proc. Fourth Thematic Conf. Remote Sensing for Marine and Coastal Environ*., Ann Arbor, MI: Environmental Research Institute of Michigan, 1997, **I**, 381–385.

Piskozub, J., V. Drozdowska, and V. Varlamov, A lidar system for remote measurement of oil film thickness on sea surface. In *Proc. Fourth Thematic Conf. Remote Sensing for Marine and Coastal Environ*., Ann Arbor, MI: Environmental Research Institute of Michigan, 1997, **1**, 386–391.

Pogorzelski, S.J., Ultrasound scattering for characterization of marine crude oil spills. In *Encyclopedia of Environmental Control Technology*, Houston, TX: Gulf Publishing Company, 1995, 485–537.

Poitevin, J. and C. Khaif, A numerical study of the backscattered radar power in presence of oil slicks on the sea surface. In *Proc. First Thematic Conf. Remote Sensing for Marine and Coastal Environ*., Ann Arbor, MI: ERIM Conferences, 1992, 171–182.

Rand, R.S., D.A. Davis, M.B. Satterwhite, and J.E. Anderson, Methods of monitoring the Persian Gulf oil spill using digital and hardcopy multiband data. U.S. Army Corps of Engineers Report, TEC-0014, 1992, 33.

Reimer, E.R. and J.R. Rossiter, Measurement of oil thickness on water from aircraft; A: Active microwave spectroscopy; B: Electromagnetic thermoelastic emission. Environmental Studies Revolving Fund Report Number 078, Ottawa, ON, 1987.

Remotec Applications Ltd., Laboratory experiments in the detection of oil under ice. Environment Canada Manuscript Report EE-26, Ottawa, ON, 1981.

Rogne, T.J. and A.M. Smith, *Tenyo Maru* oil spill remote sensing data analysis. Washington, DC: Marine Spill Response Corporation, MSRC Technical Report Series 92-003, 1992, 97.

Rogne, T., I. Macdonald, A. Smith, M.C. Kennicutt, and C. Giammona, Multi-spectral remote sensing and truth data from the *Tenyo Maru* oil spill. In *Proc. First Thematic Conf. Remote Sensing for Marine and Coastal Environ*., Ann Arbor, MI: ERIM Conferences, 1992, 37–48. (Also published in *Photogrammetric Engineering and Remote Sensing*, 1993, **59**(3), 391–397.)

Salisbury, J.W., D.M. D'Aria, and F.F. Sabins, Thermal infrared remote sensing of crude oil slicks. *Remote Sensing in the Environ*., 1993, **45**, 225–231.

Schriel, R.C., Operational air surveillance and experiences in the Netherlands. In *Proc. 1987 Intl. Oil Spill Conf*., Washington, DC: American Petroleum Institute, 1987, 129–136.

Seakem Oceanography, Remote sensing chronic oil discharges. Environment Canada Manuscript Report EE-108, Ottawa, ON, 1988, 46.

Skou, N., B.M. Sorensen, and A. Poulson, A new airborne dual frequency microwave radiometer for mapping and quantifying mineral oil on the sea surface. In *Proc. Second Thematic Conf. Remote Sensing for Marine and Coastal Environ*., Ann Arbor, MI: ERIM Conferences, 1994, II-559–565.

Solberg, R. and N. Theophilopoulos, ENVISYS — a solution for automatic oil spill detection in the Mediterranean. In *Proc. Fourth Thematic Conf. Remote Sensing for Marine and Coastal Environ*., Ann Arbor, MI: Environmental Research Institute of Michigan, 1997, **I**, 3–12.

Stapleton, G.F., S.K. Parashar, J.B. Snellen, and R.D. Worsfold, Detection of oil under ice — a laboratory program. In *Proc. Fourth Annual Arctic Marine Oilspill Program Tech. Sem.*, Ottawa, ON: Environment Canada, 1981, 587–605.

Süss, H., K. Grüner, and W.J. Wilson, Passive millimeter wave imaging: A tool for remote sensing. *Alta Frequenza*, 1989, **LVIII**(5–6), 457–465.

Taft, D.G., D.E. Egging, and H.A. Kuhn, Sheen surveillance: An environmental monitoring program subsequent to the 1989 *Exxon Valdez* shoreline cleanup. In *Exxon Valdez Oil Spill: Fate and Effects in Alaskan Waters*, ASTM STP 1219, Philadelphia, PA: American Society for Testing and Materials, 1995, 215–238.

Taylor, S., 0.45 to 1.1 μm Spectra of Prudhoe crude oil and of beach materials in Prince William Sound, Alaska. CRREL Special Report No. 92–5, Cold Regions Research and Engineering Laboratory, Hanover, NH, 1992, 14.

Tennyson, E.J., Shipborne radar as an oil spill tracking tool. In *Proc. Eleventh Arctic and Marine Oilspill Program Tech. Sem.*, Ottawa, ON: Environment Canada, 1985, 385–390.

Tunaley, J.K.E., The scattering of electromagnetic waves from the sea-ice oil and sea-water interfaces. In *Proc. Eighth Annual Arctic Marine Oilspill Program Tech. Sem.*, Ottawa, ON: Environment Canada, 1985, 292–302.

Tunaley, J.K.E. and D.R. Moorcroft, Aspects of the detection of oil under sea ice using radar methods. In *Proc. Ninth Annual Arctic Marine Oilspill Program Tech. Sem.*, Ottawa, ON: Environment Canada, 1986, 463–474.

Ulaby, F.T., R.K. Moore, and A.K. Fung, *Microwave Remote Sensing: Active and Passive*, Norwood, MA: Artech House Inc., 1989, 1466–1479.

Voloshina, I.P. and O.Y. Sochnev, Observations of surface contamination of the region of the Kol'shii Gulf from IR measurements. *Soviet J. Remote Sensing*, 1992, **9**(6), 996–1000.

Wadsworth, A., W.J. Looyen, R. Reuter, and M. Petit, Aircraft experiments with visible and infrared sensors. *Intl. J. Remote Sensing*, 1992, **13**(6–7), 1175–1199.

Wahl, T., K. Eldhuset, and Å. Skøelv, Ship traffic monitoring and oil spill detection using ERS-1. In *Proc. Intl. Symp. Operationalization of Remote Sensing*, ITC Enschede, The Netherlands, 1993, 97–105.

Werle, D., B. Tittley, E. Theriault, and B. Whitehouse, Using Radarsat-1 SAR imagery to monitor the recovery of the *Irving Whale* oil barge. In *Proc. Intl. Symp: Geomatics in the Era of Radarsat*, Ottawa, ON, 1997.

Wiese, F.K., Seabirds and Atlantic Canada's ship-source oil pollution: Impacts, trends, and solutions. World Wildlife Fund Canada Contract Report, 2002, 85.

Wiese, F.K. and P.C. Ryan, The extent of chronic marine oil pollution in Southeastern Newfoundland waters assessed through beached bird surveys 1984–1999. *Mar. Poll. Bull.*, 2003, **46**, 1090–1101.

Wiese, F.K., G.J. Robertson, and A.J. Gaston, Impacts of chronic marine oil pollution and the Murre Hunt in Newfoundland on thick-billed Murre *Uria lomvia* populations in the Eastern Canadian Arctic. *Biol. Conserv*., 2004, **116**, 205–216.

Yan, X-H. and P. Clemente-Colon, The maximum similarity share matching (MSSM) method applied to oil spill feature tracking observed in SAR imagery. In *Proc. Fourth Thematic Conf. Remote Sensing for Marine and Coastal Environ*., Ann Arbor, MI: Environmental Research Institute of Michigan, 1997, **I**, 43–55.

Zhifu, S. and W. Wiesbeck, A study of passive microwave remote sensing. In *Proc. 1988 Intl. Geoscience and Remote Sensing Symp*., European Space Agency, Paris, France, 1988, 1091–1094.

Zielinski, O. and N. Robbe, Past and future of airborne pollution control. In *Proc. Interspill*, Trondheim, Norway, 2004.